

Design and Development of an Accelerated Material Synthesis Platform for Automated Materials Research

by
Eunice I. Aissi

Submitted to the Department of Mechanical Engineering
in partial fulfillment of the requirements for the degree of
MASTER OF SCIENCE IN MECHANICAL ENGINEERING

at the
MASSACHUSETTS INSTITUTE OF TECHNOLOGY

September 2024

© 2024 Eunice I. Aissi. This work is licensed under a [CC BY-NC-ND 4.0](#) license.

The author hereby grants to MIT a nonexclusive, worldwide, irrevocable, royalty-free license to exercise any and all rights under copyright, including to reproduce, preserve, distribute and publicly display copies of the thesis, or release the thesis under an open-access license.

Authored by: Eunice I. Aissi
Department of Mechanical Engineering
August 23, 2024

Certified by: Tonio Buonassisi
Professor of Mechanical Engineering, Thesis Supervisor

Accepted by: Nicolas Hadjiconstantinou
Chairman, Department Committee on Graduate Theses

Design and Development of an Accelerated Material Synthesis Platform for Automated Materials Research

by

Eunice I. Aissi

Submitted to the Department of Mechanical Engineering
on August 23, 2024 in partial fulfillment of the requirements for the degree of

MASTER OF SCIENCE IN MECHANICAL ENGINEERING

ABSTRACT

Materials development is the foundation for innovation in many industries and fields, however, this process is traditionally slow and resource-intensive. Most often, new materials are developed and characterized on the time scale of years which can limit the pace of scientific and industry innovation. I address the material synthesis and characterization bottleneck by presenting a framework that I believe is suitable for smaller labs: Self-built, low-cost automation. The design philosophy is to de-risk the lab automation process by keeping costs low, failing fast, and leveraging common resources in electronic systems and additive manufacturing. I present an improved version of a low-cost but high-throughput ink-jet material printer developed by Siemenn *et al.* and adapted to operation in the glovebox, hood, and benchtop environments. The tool is capable of depositing gradients of droplets with unique compositions at a rate of up to 1000 materials per minute, is self-built and cost around \$500. I also present a computer-vision-enabled high-throughput material characterization algorithm for stability quantification through color degradation. The synthesis and characterization methods are validated on a methylammonium lead iodide (MAPbI₃) and formamidinium lead iodide (FAPbI₃) perovskite material system. X-ray diffraction (XRD), X-ray photoelectron spectroscopy (XPS), and hyperspectral imaging measurements show equivalence between high-throughput synthesis and more traditional spin-coating methods. Results obtained through the high-throughput stability characterization method are aligned with stability trends reported in literature and has an accuracy of 96.9% when compared to ground-truth degradation as measured by a domain expert.

Thesis supervisor: Tonio Buonassisi

Title: Professor of Mechanical Engineering

Acknowledgments

I would like to express my deepest appreciation to my Advisor Tonio Buonassisi for his professional guidance, feedback and support. I'm also extremely grateful to Alexander E. Siemenn and Basita Das for their mentorship and continued belief in my potential. Additionally, this endeavor would not have been possible without the generous support from First Solar, who partially funded the work presented in this thesis.

I could not have undertaken this journey without my undergraduate advisor Russell Scott Ray who mentored me and introduced me to the world of academia and my classmate and, at times teacher, Fang Sheng for her support and instruction.

Lastly, but definitely not least, words cannot express my gratitude to my family and partner who supported me and lifted me up when I doubted myself.

Contents

<i>List of Figures</i>	9
<i>List of Tables</i>	13
1 Introduction	15
1.1 Motivation	15
1.2 An overview of the Archerfish Material Printer	16
1.3 Thesis Overview	17
2 Improving Archerfish: Advancements in Communication Protocols and Hardware	19
2.1 Introduction and Overview	19
2.2 Improvements to the Communications Architecture	20
2.3 Hardware Updates: Enhancing Droplet Uniformity, and Crystallization	21
2.4 Successes in Printing Organic Perovskite Materials	23
2.4.1 Methods	24
2.5 Chapter Summary	25
3 High - Throughput Characterization of Perovskite Materials	27
3.1 Introduction and Overview	28
3.2 Detecting Perovskite Degradation from RGB Time Series Data	28
3.2.1 Segmentation and Identification of Droplets	28
3.2.2 Color Calibration	29
3.2.3 Composition Extraction	30
3.2.4 Instability Calculation	31
3.3 Results	32
3.4 Chapter Summary	34
4 Limitations of the Platform	35
4.1 Introduction and Overview	35
4.2 Lack of Compositional Control	35
4.3 Droplet Generation	37
4.4 Environmental and Crystallization Control	38
4.5 Unknown Mixing Mechanisms	39
4.6 Other Limitations	41
4.6.1 Material Compatibility	41
4.6.2 Human Introduced Variation	41

4.6.3	Lack of System Feedback	42
4.7	Chapter Summary	42
5	Conclusion	43
5.1	Summary	43
5.2	Future Work	43
A	Archerfish Components List	45
B	Archerfish Raspberry Pi Code	47
C	Archerfish Arduino Code	65
	<i>References</i>	73

List of Figures

1.1	The Archerfish platform, is a retrofitted 3D printer that can deposit gradients of droplets at a rate of up to 1000 droplets a minute. It consists of two home-built 3 ml syringe pumps which dispense streams of fluid that join at a y-junction and are generated into droplets by a Lee valve forcing flow through a 300 μm diameter ceramic nozzle. Note that the fluid inlets from the syringe pumps are marked by a + sign.	16
1.2	The Archerfish syringes are driven by \$3 28BYJ- 48 stepper motors coupled to a 4-40 lead screw to force the plunger forward and dispense fluid. The motors create a fluid gradient from 100% of the fluid in syringe B controlled by motor B to 100% of the fluid in syringe A controlled by motor A using a descending and ascending speed profiles respectively. Note that the fluid outlets from the syringe pumps are marked by a + sign.	17
2.1	The second iteration of Archerfish was developed to address the chemical limitations of the initial proof of concept. Mainly, the system was fitted with wireless communication and a GUI for use with lead containing perovskites inside a glovebox.	19
2.2	The flow diagram for the Archerfish system’s Graphical User Interface (GUI).	20
2.3	The flow diagram for the Archerfish system’s Graphical User Interface (GUI) with screenshots of the three main screens. The first screen is used to choose the type of experiment the user is running, next the set-up screen asks for experimental details including precursor names and saves this information for experimental logging. This screen also includes a hardware control interface to load the syringe pumps and changes its input fields based on the experiment type and the number of pumps being used. Lastly, a simple glove-box window with prominent start and stop buttons allow the user to control the printer while working in an enclosed environment with limited mobility. Note that the GUI adapts its configuration to the type of experiment and the number of syringe pumps being used for each experiment.	22
2.4	A New 3D printed casing was designed to hold an external pinch valve and the dispensing nozzle for improved droplet uniformity.	23
2.5	a) Thermal non-uniformity observed through infrared imaging of a commercial hotplate initially used to anneal Archerfish perovskite samples. b) The new hotplate built in lab shows better uniformity than its commercial counterpart.	24

2.6	FAPbI ₃ - MAPbI ₃ hybrid organic-inorganic perovskite droplets printed using the Archerfish system where characterized using X-ray diffraction (XRD), X-ray photoelectron spectroscopy (XPS), and hyperspectral imaging. (b) A $\Delta 2\theta$ of 0.152 deg occurs in an XRD peak corresponding in a change of composition from MAPbI ₃ to FAPbI ₃ . (c) Similarly, a change in the peak corresponding to the $C = NH_2$ double bond found in formamidinium indicates a gradient from MAPbI ₃ to FAPbI ₃ . (d) Lastly, a gradual change in the reflectance spectra of the droplets obtained using hyperspectral imaging indicate a change in composition from pure MAPbI ₃ to FAPbI ₃ . This figure and its measurements are reproduced with permission from Siemenn and Aissi <i>et al.</i> [8], the measurements where taken by Fang Sheng and Alexander Siemenn.	25
3.1	a-c Automatic degradation testing and measurement of computer vision-segmented perovskite deposits. a , The samples are placed in the degradation chamber with specified environmental conditions for a total of two hours. b , RGB images of the samples are taken every 30 seconds for two hours to resolve the time-dependent color change in material. c , Computer vision is used to segment each deposited sample over time, $\Phi(t)$, to compute the degradation intensity metric, I_c . This figure reproduced with permission from Siemenn and Aissi <i>et al.</i> [8]	27
3.2	a) The droplets on the glass substrate cropped out of the first image in the series. b) Each droplet is identified and labeled as the output of the watershed image segmentation algorithm.	29
3.3	a) The cropped image of the perovskite droplets before it is processed by the color-calibration algorithm. b) The same image post calibration, note that the true color of droplets are now accessible and the purple hue created by the illumination conditions have been rectified.	30
3.4	The first step in composition extraction is determining the corners of the glass substrate onto which the droplets are printed. This is done through a series of computer vision morphological operations and algebraic representations.	31
3.5	The second step in composition extraction is a perspective transform to obtain a bird's eye view of the droplets. a) This row provides the results of the perspective warp on all the Archerfish droplets. b) In this row, the same droplet is highlighted in yellow to indicating the retention of spatial information for each droplet, the yellow droplet appears in the same position relative to other droplets in both the initial and the warped perspectives.	32
3.6	An example of a time series color change of every droplet in a sample. Each horizontal line represents the color of a droplet along the FA _{1-x} MA _x PbI ₃ ($0 \geq x \geq 1$) compositional gradient over the degradation experiment.	32

3.7	<p>a, Performance of the autocharacterization of degradation intensity, I_c, relative to the ground truth degradation determined by a domain expert (yellow scatter points) on $N = 201$ unique perovskite samples across 3 independent trials. The black dashed line indicates the split between high and low I_c values, corresponding to high and low degrees of degradation, respectively.</p> <p>b, Images of the three batches of $\text{FA}_{1-x}\text{MA}_x\text{PbI}_3$ gradient samples after the 2-hour controlled degradation. The leftmost samples are FA-rich and the rightmost samples are MA-rich. The yellowed FA-rich compounds have undergone a phase transition from $\alpha\text{-FAPbI}_3$ to $\delta\text{-FAPbI}_3$ and are considered as "ground truth" degradation samples if they exhibit a deviation of $> 0.02\text{eV}$ in band gap from pre- to post-degradation, evaluated by a domain expert. This figure reproduced with permission from Siemenn and Aissi <i>et al.</i> [8]</p>	33
4.1	<p>Energy-dispersive X-ray spectroscopy (EDS) elemental composition traces. These elemental traces are shown for a $\text{Cs}_3\text{Bi}_2\text{I}_9\text{-Cs}_3\text{Bi}_2\text{Br}_9$ (cesium bismuth iodide-cesium bismuth bromide) perovskite gradient printed using Archerfish where each droplet has its EDS spectrum measured. We note the abrupt stop in the compositional shift between iodine and bromine due to improper tuning of the Archerfish print settings. Approximately 80% of the entire gradient is shown to be successfully printed here, the missing portion of the gradient is visualized using dashed line projections. This figure reproduced with permission from Siemenn and Das <i>et al.</i> [20]</p>	36
4.2	<p>The measured flow rate from the current \$10 Archerfish syringes with a constant motor speed. Large and small oscillatory spikes with magnitudes of up to 333% of the set flow rate occur periodically due to the rotation of the stepper motor. The x-axis is in 20 second intervals.</p>	37
4.3	<p>Results of a flow rate measurement test indicates non-linearities in the expected flow rate due to a pressure build-up effect. The syringe was refilled between the data points circled in red, despite an increase in the motor speed, the flow rate after a refill remains nearly the same. This effect is a result the rubber plunger in the syringe relaxing when drawing in fluid and therefore needing to re-pressurize before any fluid is dispensed.</p>	38
4.4	<p>The profile of a droplet along the $\text{Cs}_3\text{Bi}_2\text{Br}_9$ to $\text{Cs}_3\text{Sb}_2\text{I}_9$ perovskite gradient obtained through stylus profilometry. A coffee ring affect can be seen, with high ridges along the edge of the droplet and a near-flat film in the middle.</p>	39
4.5	<p>Two different Archerfish prints of the same $\text{FAPbI}_3\text{-MAPbI}_3$ compositional gradient after annealing and controlled degradation. Yellow samples are degraded while black samples are not degraded. These two perovskite gradients exhibit different degradation patterns despite being of the same composition and degrading under the same conditions. The differences in crystallization, as shown by the SEM images, transpired from spatial non-uniformities in the annealing and deposition processes. This figure reproduced with permission from Siemenn and Das <i>et al.</i> [20]</p>	40

4.6	Optical microscope images through a machined acrylic 4-way junction with 1/32" inner diameters fluid paths of a) the point of fluid stream contact with clear separation and no mixing and b) the inlet to the droplet generator indicating, as expected, that no mixing occurs when the fluid streams meet. The arrows indicate the direction of flow.	41
4.7	Optical microscope images through a machined acrylic three-way junction with inlets at 90 degrees. RGB color analysis show mixing at the outlet of the old Archerfish Lee valve, suggested that agitation via the valve could be a viable path to achieve known mixing for Archerfish droplets. Figure reproduced with permission from Siemenn and Das <i>et al.</i> [20]	42

List of Tables

A.1	General component list for the improved Archerfish system. Detailed bill of materials and building instructions for version one of the Archerfish Platform are provided by Siemenn <i>et al.</i> [20]	45
-----	---	----

Chapter 1

Introduction

1.1 Motivation

Automation in research is a growing field that has recently gained attention for its potential to accelerate and improve the quality of scientific outcomes.[1] However, acquiring the human and capital resources to establish and maintain these advanced tools can be daunting. For smaller labs investigating a wide range of energy materials, there is demand for low-cost, flexible, high-throughput (HT), and high-quality materials synthesis and characterization tools.

In this thesis, I develop low-cost high-throughput synthesis and characterization methods for automated materials exploration. I present an improved version of a low-cost but high-throughput ink-jet material printer developed by Siemenn *et al.* [2] and adapted to operation in the glovebox, hood, and bench-top environments. The printer takes two or more fluid precursors and prints a materials gradient within a set of droplets, line segments, or another user-specified shape. The tool is self-built, leveraging a low-cost 3D printer chassis, and is affordable at about \$500. Our build cycle takes one day and utilizes open-source platforms for its firmware. The printer can deposit up to 1,000 different material compositions in under one minute and is easy to use, requiring only three steps: creating a print pattern, loading the precursors, and printing the materials.

One area of interest for accelerated materials discovery is perovskite materials, compounds of structure ABX_3 , where A and B are cations and X is a non metallic anion, that can be used as solar cell materials.[3] The perovskite crystal structure was first discovered in 1839[4] and since then a subset of these materials know as metal halide perovskites have shown great promise in optoelectronic applications such as LEDs, lasers, and solar cells. [5] Metal halide perovskite solar cells have been reported to reach power conversion efficiencies as high as 26.1% while being light weight and easy of synthesise. [6] However, they currently suffer from low stability and can degrade quickly when exposed to irradiation and heat. [7] This limits their applicability as solar cell materials and has slowed their adoption. Consequently, there has been great interest in optimizing and discovering perovskite solar cell ink formulas to both improve their stability and understand their modes of degradation. The material space is however vast for both composition and additives making it a suitable materials system for exploration through high-throughput combinatorial material synthesis.

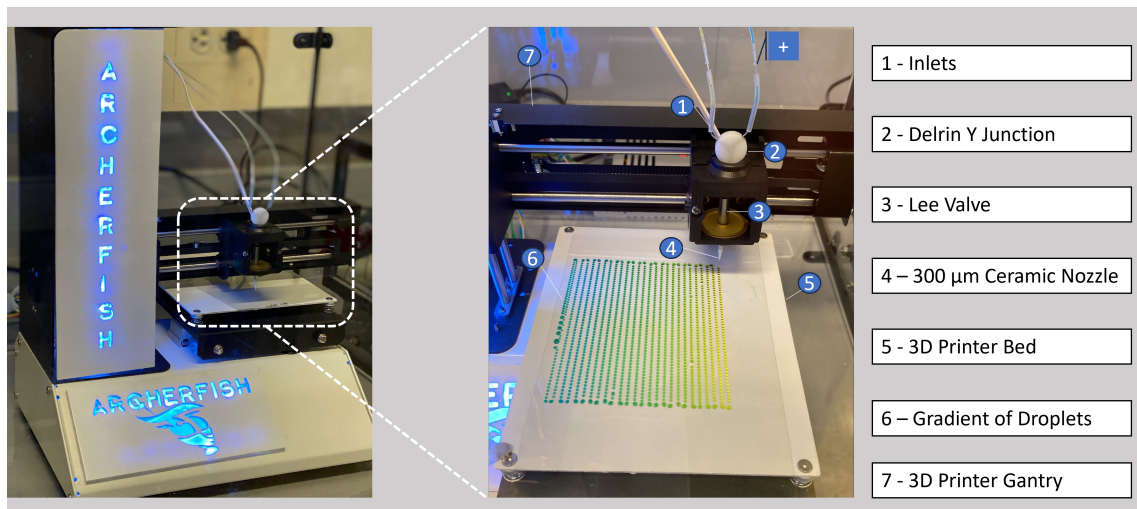


Figure 1.1: The Archerfish platform, is a retrofitted 3D printer that can deposit gradients of droplets at a rate of up to 1000 droplets a minute. It consists of two home-built 3 ml syringe pumps which dispense streams of fluid that join at a y-junction and are generated into droplets by a Lee valve forcing flow through a 300 μm diameter ceramic nozzle. Note that the fluid inlets from the syringe pumps are marked by a + sign.

I therefore validate the material-synthesis capacity of the methods I develop in this thesis on the methylammonium lead iodide (MAPbI_3) and formamidinium lead iodide (FAPbI_3) perovskite material system by showing equivalence to traditional spin-coated samples through X-ray diffraction, X-ray photoelectron spectroscopy (XPS), and hyperspectral imaging measurements. I also demonstrate high-throughput characterization of the perovskite materials through an algorithm that quantifies color changes in each material as a proxy for material degradation. In summary, I present and validate a framework of customized automation focused on improving R&D reproducibility and speed for smaller academic labs.

1.2 An overview of the Archerfish Material Printer

The Archerfish platform illustrated in Figure 1.1 was first invented by Alexander Siemenn and James Serdy in the Accelerated Materials Development for Sustainability Lab. [2]. Archerfish is a low-cost and high-throughput droplet deposition system that can create gradients of droplets at a rate of up to 1000 droplets per minute. In the first version of this platform, the plungers of two 3 ml syringes were replaced with a 4-40 lead screw and actuated with 28BYJ-48 stepper motors and ULN2003 drivers. These home-built pumps were controlled via an Arduino board in the ascending and descending stair-case flow pattern in Figure 1.2. The two streams from each pumps were then joined in a spherical y-joint machined from delrin and ink-jetted through a piezoelectric lee valve and out of a 300 μm ceramic nozzle. Lastly, the nozzle of a Monoprice MP select Mini Pro 3D printer was removed and replaced with the droplet generator to deposit the droplets at locations specified by the g-code uploaded to the printer. With this design, researchers at the Accelerated Materials development lab were able to create a high-throughput materials synthesis platform for use with simple solution

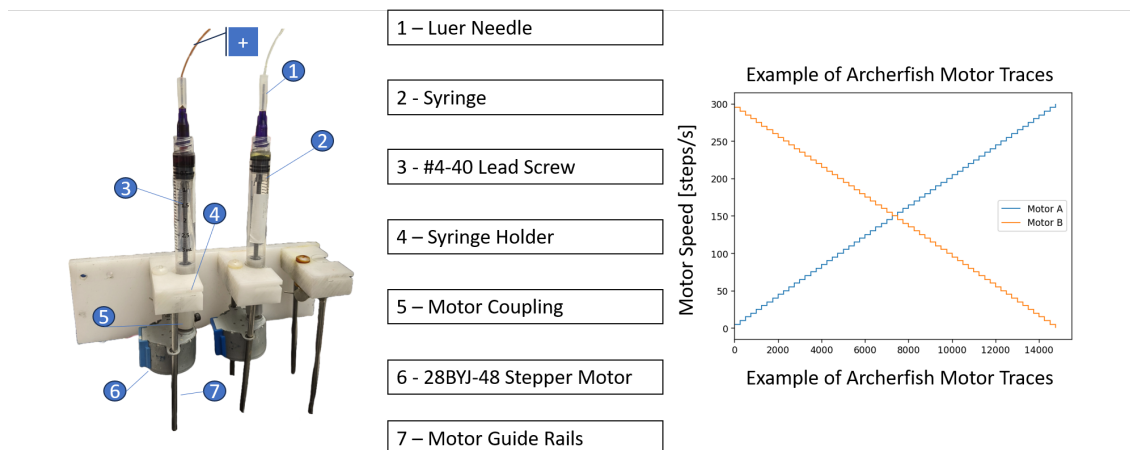


Figure 1.2: The Archerfish syringes are driven by \$3 28BYJ- 48 stepper motors coupled to a 4-40 lead screw to force the plunger forward and dispense fluid. The motors create a fluid gradient from 100% of the fluid in syringe B controlled by motor B to 100% of the fluid in syringe A controlled by motor A using a descending and ascending speed profiles respectively. Note that the fluid outlets from the syringe pumps are marked by a + sign.

based chemistries. However, the system had several limitations included a lack of proper communications protocols that prevented it from being used in environmental enclosures such as a glove box, a near necessity for experiments with lead containing perovskites.

1.3 Thesis Overview

This master’s thesis designs and develops improved high-throughput material synthesis and characterization platforms and algorithms to accelerate the discovery of novel energy materials.

Redesigning the Archerfish High-Throughput (HT) Platform: In order to allow for a wider range of material experiments, I implement several improvements to the communications and hardware components of the Archerfish platform. Chapter 2 describes these improvements to the Archerfish system’s hardware and electronic components while motivating and explaining design choices.

Algorithms for HT Characterization: HT synthesis without characterization limits the pace of materials discovery. Chapter 3 describes an algorithm I developed to extract a key material property of perovskite materials, stability, printed using a high-throughput droplet deposition system like Archerfish.

Limitations of The Archerfish System: Despite its potential, the Archerfish platform is still imperfect. Chapter 4 describes its limitations and potential pathways to further improvements.

Chapter 2

Improving Archerfish: Advancements in Communication Protocols and Hardware

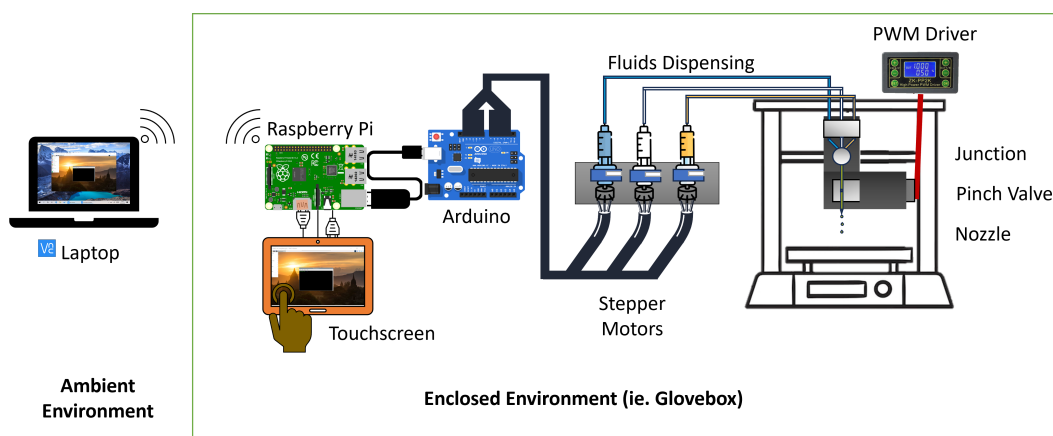


Figure 2.1: The second iteration of Archerfish was developed to address the chemical limitations of the initial proof of concept. Mainly, the system was fitted with wireless communication and a GUI for use with lead containing perovskites inside a glovebox.

2.1 Introduction and Overview

Section 1.2 describes the proof of concept version of Archerfish first designed by Siemenn *et al.* [2], however, it needed several updates in order to be utilized for chemical experiments. In this chapter I describe the updates I implemented for the communications, user interface, and aspects of the hardware in order to allow us to run chemical experiments in an inert environment. These updates to version one of Archerfish system are depicted in Figure 2.1.

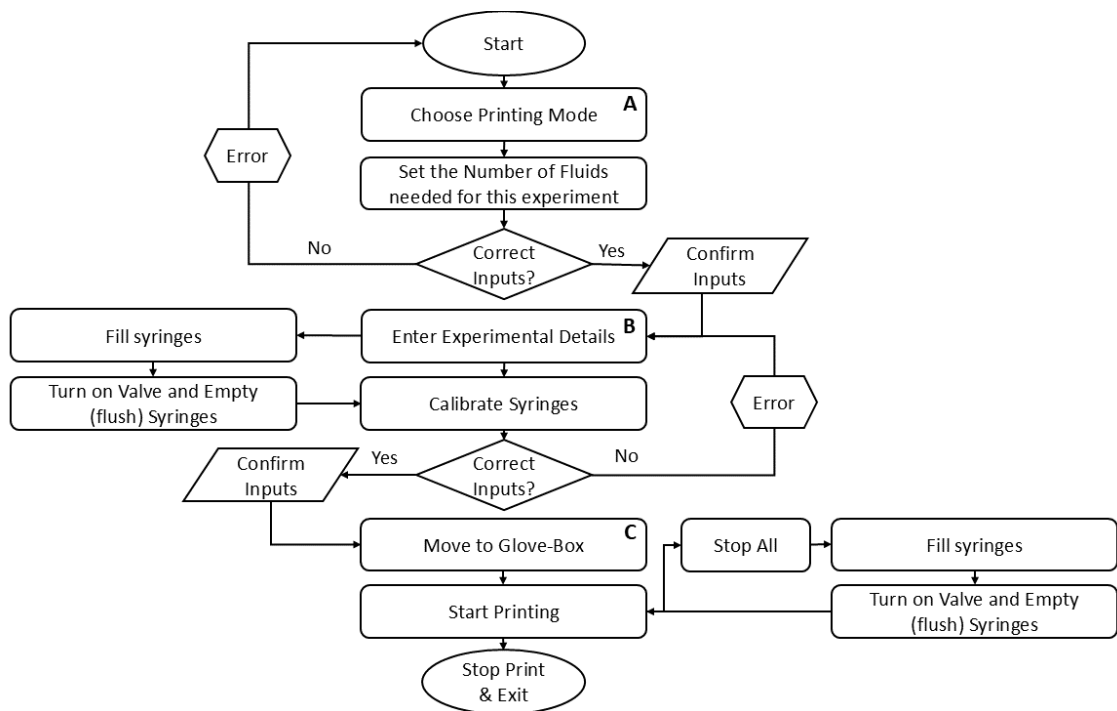


Figure 2.2: The flow diagram for the Archerfish system’s Graphical User Interface (GUI).

2.2 Improvements to the Communications Architecture

The primary limitation of the Archerfish system was its communications architecture. Originally it utilized prescribed printing flow rates for each syringe and a set deposition pattern that could be activated once the machine was turned on. To change precursors, the user had to remove the syringe pump motors and mount a smaller pump pre-programmed to move in reverse and draw in liquid. This meant that there was no way to easily change precursors, the composition of the gradient, how many droplets were printed, or where the droplets were deposited. Chemical experiments, however, require flexibility for composition and deposition as well as peripheral features like data logging. Moreover, chemical synthesis needed to occur in an enclosed environment such as a glove box where users had limited mobility and dexterity due to bulky chemical safety gloves. Features that required fine movements for reoccurring actions such as exchanging a motor to reload precursors were therefore intractable.

To allow for more flexibility, a Raspberry Pi was added as a control center to run a Graphical User Interface (GUI). The pi can be controlled wirelessly from outside the glove box via a bluetooth connection to a Virtual Network Computing (VNC) client. The VNC mirrored the raspberry pi screen on a laptop outside the glove box, allowing a user to set printing parameters through the GUI and control the hardware inside the glove box. Once the user connects to the raspberry pi, they are instructed to choose one of three printing modes: batch, two-fluid gradient, and constant+ two-fluid gradient. The pi then establishes a connection with the arduino and sends motor control instructions via serial communication to set the flow rates for the syringe pumps.

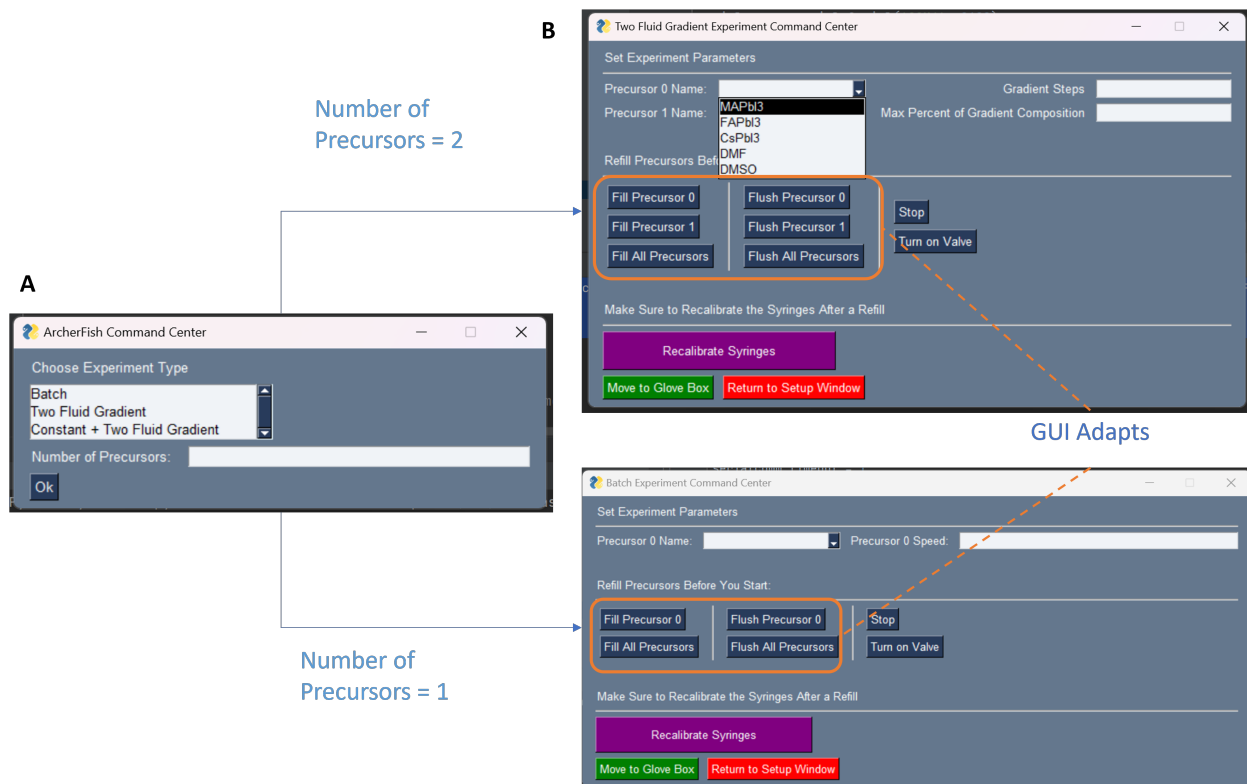
In batch mode, the relative flow rates of each syringe pump is set by the user in the GUI, the printed droplets are therefore multiple copies of the same composition. In two-fluid gradient mode, the flow rates of two syringe pumps change from a starting percentage of one precursor to a percentage of the other, creating a linear gradient between the two precursors loaded into the syringe pumps. This percentage value is chosen by the user and allows for finer resolution into sub-regions of a gradient of interest. For example, if a user notices interesting features in the regions between the droplets of composition $A_{0.25}B_{0.75}$ and the $A_{0.75}B_{0.25}$, they could specify these compositions as end points of a new gradient with all the droplets between this range, thereby zooming into this compositional space. In constant+ two-fluid gradient mode, a third syringe pump dispenses a precursor at a constant flow rate alongside the gradient adding a third component to the droplet composition, this is usually a solvent. After choosing a printing mode, the GUI asks for user inputs regarding experimental details such as the chemical names for the loaded precursors and saves these in a text file called Experimental log for later reference. Once all experimental details have been captured, the GUI goes to a simple run screen that features a prominent start and stop button. At this point, the user can enter the glove-box space using the bulky protective glove-box gloves and any further interactions with the Archerfish system takes place on the touch screen inside. The touchscreen is to facilitate use of the system and features two large start and stop buttons that can be pressed even with the bulky gloves that decrease the dexterity of the user.

It is important to note that the GUI also guides the user with confirmation and error messages to ensure that all necessary data is properly captured and the user follows the proper path through the GUI. The full GUI path is shown in Figure 2.2 and images of the three main windows along the path are shown in Figure 2.3. The GUI windows are dynamic and adaptable to each experimental set-up, they change their input fields depending on the type of print and the number of fluids the experiment requires.

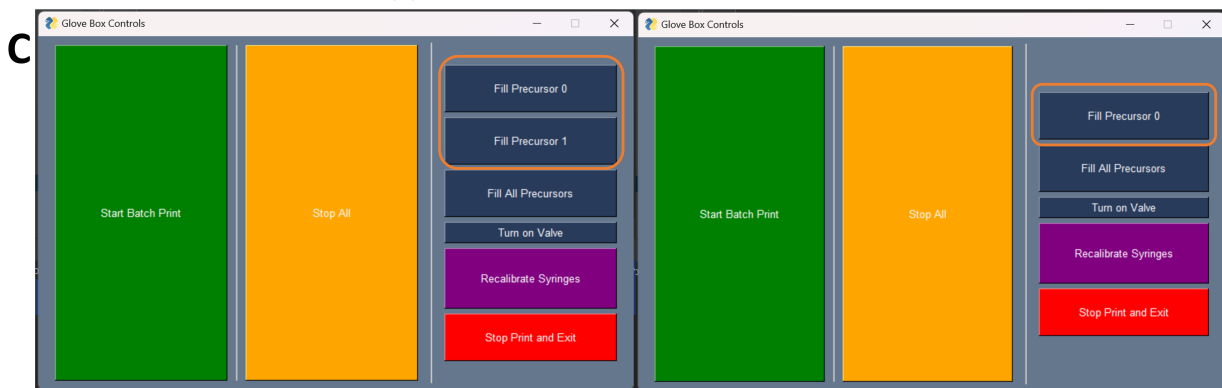
2.3 Hardware Updates: Enhancing Droplet Uniformity, and Crystallization

Beyond the flexibility of the system, two challenges limited our ability to print gradients of perovskite droplets: droplet uniformity, and uniform annealing. Test prints revealed that the unknown internal volume of the initial Archerfish Lee valve resulted in reservoirs of trapped fluid that required large volumes of transfer fluid to completely clear out. The unknown chemical composition of the wetted materials also created a potential for side reactions that could adversely impact the deposited materials purity. Consequently, the lee valve was replaced with a 24 V Precigenome solenoid pinch valve to provide breaks in the outlet fluid stream and generate droplets. Unlike the lee valve, the pinch valve’s surfaces are not wetted, the actuator strikes a 1/32" ID x 3/32" OD silicone tube containing outlet fluid in a square wave pattern. A new 3D printed casing shown in Figure 2.4 was designed to hold the valve and the nozzle steady while printing as this was shown to minimize satellite droplets and improve droplet uniformity.

Annealing is a crucial step for perovskite crystallization and therefore requires a uniform



(a) First two windows in the GUI.



(b) Last window of the GUI.

Figure 2.3: The flow diagram for the Archerfish system’s Graphical User Interface (GUI) with screenshots of the three main screens. The first screen is used to choose the type of experiment the user is running, next the set-up screen asks for experimental details including precursor names and saves this information for experimental logging. This screen also includes a hardware control interface to load the syringe pumps and changes its input fields based on the experiment type and the number of pumps being used. Lastly, a simple glove-box window with prominent start and stop buttons allow the user to control the printer while working in an enclosed environment with limited mobility. Note that the GUI adapts its configuration to the type of experiment and the number of syringe pumps being used for each experiment.

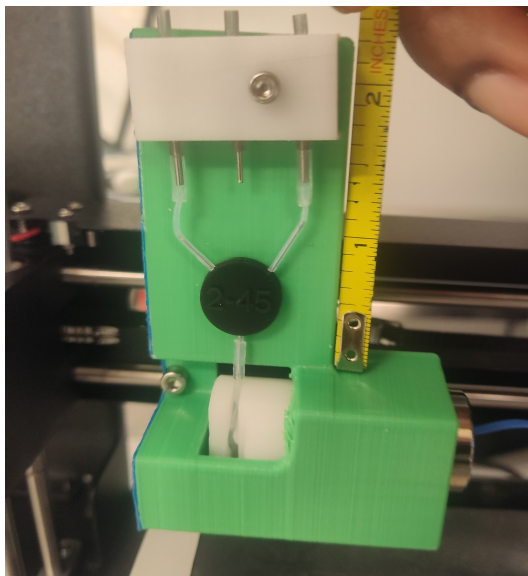


Figure 2.4: A New 3D printed casing was designed to hold an external pinch valve and the dispensing nozzle for improved droplet uniformity.

heating plate. However, infrared images of the commercial hot plate often used for chemical experiments revealed a non-uniform heating surface that resulted in noticeable degradation and poor crystallization of the perovskite droplets. Additionally, moving the samples from the print bed to the hot plate led to unpinning of the droplet edges further wetting of the glass substrate creating pools of materials instead of uniform droplets. In order to create viable perovskite samples, a new heating plate was designed and built for annealing perovskite droplets directly on the 3D printer bed and is shown in Figure 2.5. The new hot plate consisted of a flexible heating element sandwiched between a 1/8" thick glass bottom plate and an 1/8" thick aluminum top plate. Two foam pads were placed below the glass plate for structural stability. The heating element was controlled via an InkBird PID temperature controller with a k-type thermocouple for temperature feedback. Infrared images of the new heating plate revealed a near thermally uniform surface, further images were taken with a carbon sheet over the aluminum to decrease the impact of reflectance on the infrared image results. These images, though not shown here, also indicated improved thermal uniformity when compared to the commercial product.

2.4 Successes in Printing Organic Perovskite Materials

The FAPbI_3 - MAPbI_3 hybrid organic-inorganic perovskite material system was used to validate the improved Archerfish's ability to create gradients of materials in a high-throughput manner. This system was chosen because it is established with many data sets in literature that could be cross referenced for comparison with the Archerfish produced droplets. [9] Furthermore, each precursor, FAPbI_3 and MAPbI_3 , could be mixed in solution form to produce $\text{FA}_{1-x}\text{MA}_x\text{PbI}_3$ droplets with $0 \geq x \geq 1$ that could then be annealed at 150°C for 15

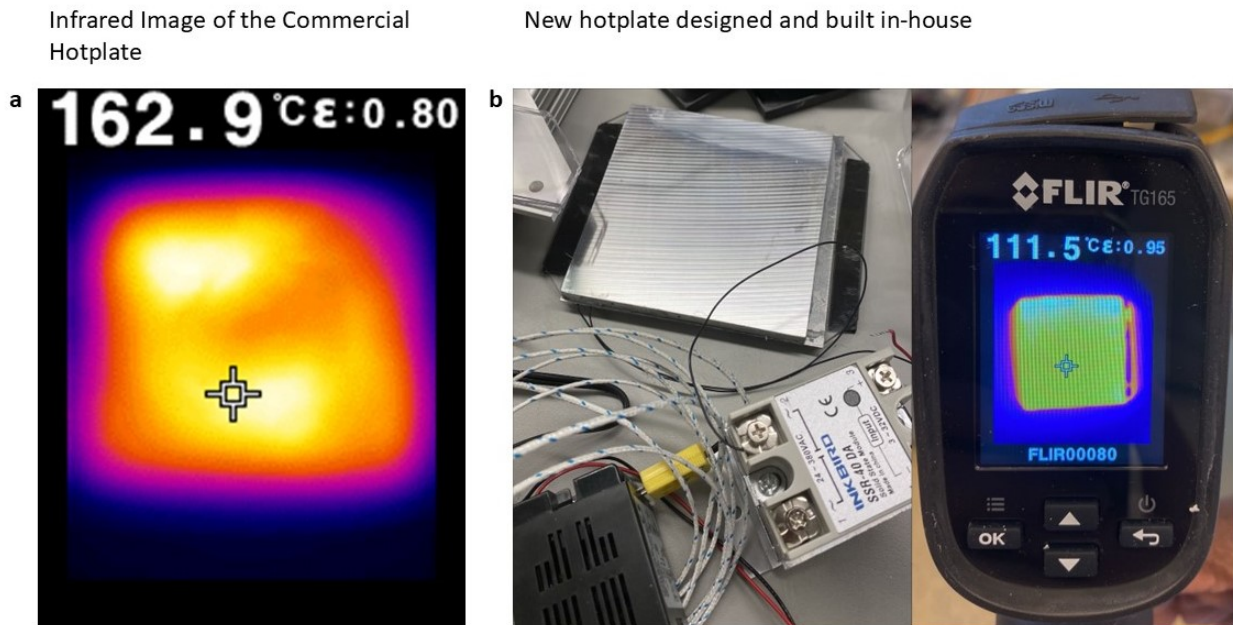


Figure 2.5: a) Thermal non-uniformity observed through infrared imaging of a commercial hotplate initially used to anneal Archerfish perovskite samples. b) The new hotplate built in lab shows better uniformity than its commercial counterpart.

minutes and crystallize to create the perovskite materials. Archerfish synthesized perovskite gradients are printed on a clean 2" \times 3" glass substrate in a serpentine pattern with the print head moving at a speed of 38 mm/s. The pinch valve actuates at 5Hz and 11% duty cycle depositing 70-80 droplets of unique compositions in roughly 16.5 seconds. Each print uses approximately 0.15ml of fluid, including fluid used to flush the lines before each print. Figure 2.6 show results of X-ray diffraction (XRD), X-ray photoelectron spectroscopy (XPS), and hyperspectral imaging that confirm the presence of a gradient across the Archerfish droplets ranging in composition from pure MAPbI₃ to FAPbI₃.

2.4.1 Methods

Materials

3" \times 2" \times 1mm glass slides (C&A Scientific) are cleaned using deionized water (DI, $< 1.0\mu\text{S}/\text{cm}$, VWR), Hellmanex III (VWR), and isopropyl alcohol (IPA, $\geq 99.5\%$, VWR) to be used as substrates. Lead iodide powder (PbI₂, 99.999% trace metal basis, Sigma-Aldrich), formamidium iodide powder (FAI, $>99.9\%$, Greatcell Solar Materials), methylammonium iodide (MAI, $>99.9\%$, Greatcell Solar Materials), dimethylformamide (DMF, $\geq 99.8\%$, Sigma-Aldrich), and dimethylsulfoxide (DMSO, $\geq 99.9\%$, Sigma-Aldrich) are used to prepare the perovskites.

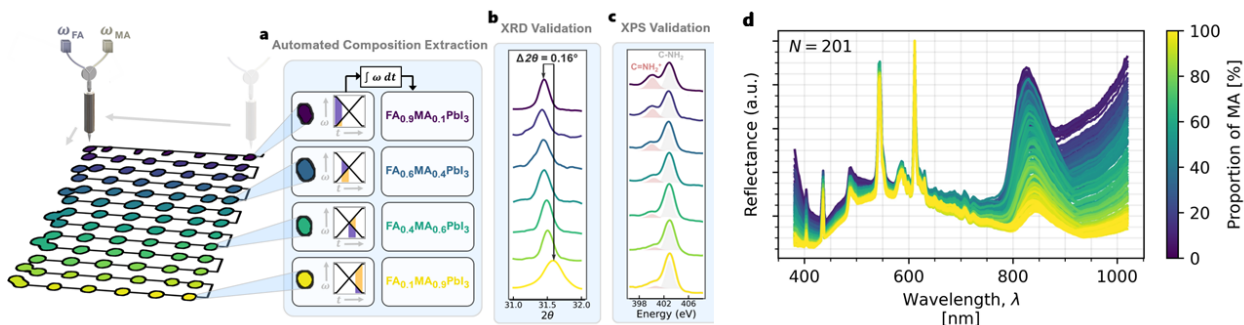


Figure 2.6: FAPbI₃ - MAPbI₃ hybrid organic-inorganic perovskite droplets printed using the Archerfish system where characterized using X-ray diffraction (XRD), X-ray photoelectron spectroscopy (XPS), and hyperspectral imaging. (b) A $\Delta 2\theta$ of 0.152 deg occurs in an XRD peak corresponding in a change of composition from MAPbI₃ to FAPbI₃. (c) Similarly, a change in the peak corresponding to the $C = NH_2$ double bond found in formamidinium indicates a gradient from MAPbI₃ to FAPbI₃. (d) Lastly, a gradual change in the reflectance spectra of the droplets obtained using hyperspectral imaging indicate a change in composition from pure MAPbI₃ to FAPbI₃. This figure and its measurements are reproduced with permission from Siemenn and Aissi *et al.* [8], the measurements were taken by Fang Sheng and Alexander Siemenn.

Substrate Preparation

Glass slide substrates are prepared for printing the perovskite samples using a three-step cleaning process: (1) ultrasonication for 5 minutes in DI water with 2%vol. Hellmanex III solution, (2) ultrasonication for 5 minutes in DI water only, and (3) ultrasonication for 5 minutes in IPA. Once cleaned, the substrates are transferred to an inert nitrogen environment glovebox with moisture levels < 10ppm.

Perovskite Preparation

FAPbI₃ (formamidinium lead iodide) and MAPbI₃ (methylammonium lead iodide) are prepared as 0.6M liquid-based precursors for high-throughput printing. For printing, 2mL of each precursor is prepared in an inert nitrogen environment glovebox with moisture levels < 10ppm. First, 3.2mL DMF is mixed with 0.8mL of DMSO to make 4mL of 4 : 1 DMF:DMSO solution. Then, 1.106g of PbI₂ powder is dissolved into the 4mL of 4 : 1 DMF:DMSO to make a PbI₂ stock. Next, the 4mL PbI₂ stock is split in half, pipetting 2mL of stock per vial. Lastly, 0.206g of FAI powder is dissolved into one of the 2mL PbI₂ stock vials and 0.191g of MAI powder is dissolved into the other making 0.6M FAPbI₃ and 0.6M MAPbI₃, respectively.

2.5 Chapter Summary

In this chapter, I present improvements to the Archerfish platform's communication protocols and hardware, then validate the capabilities of the new system by printing gradients of hybrid

organic-inorganic perovskite materials and showing compositional equivalence to spin-coated samples with XRD, XPS, and hyperspectral imaging measurements. In the next chapter, I will develop an algorithm for high-throughput characterization of materials deposited with the new Archerfish platform.

Chapter 3

High - Throughput Characterization of Perovskite Materials

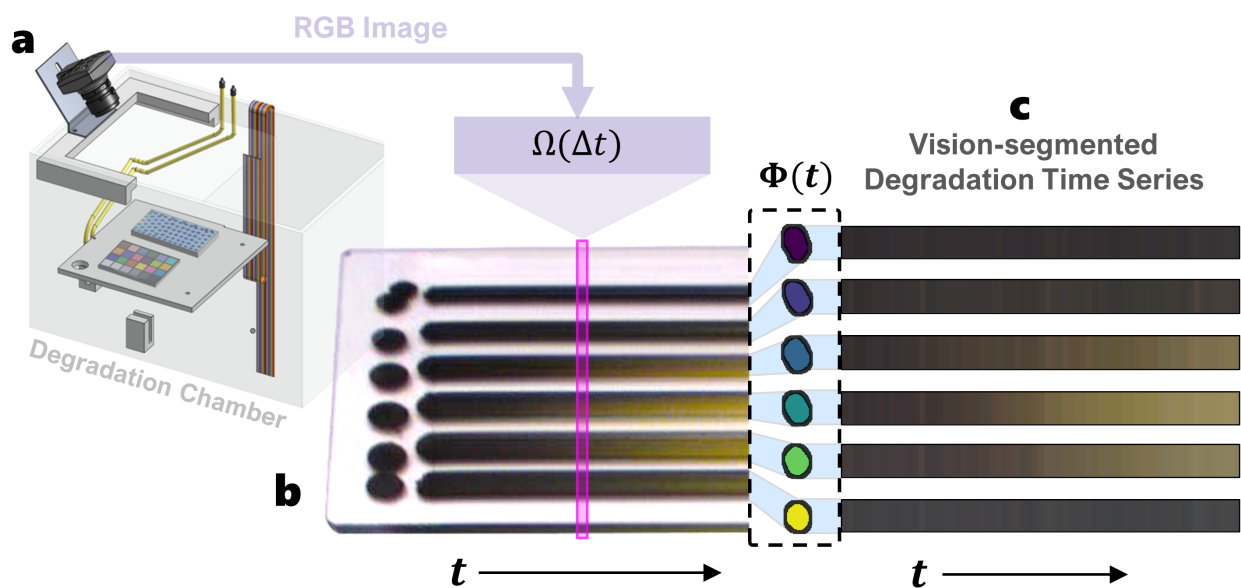


Figure 3.1: **a-c** Automatic degradation testing and measurement of computer vision-segmented perovskite deposits. **a**, The samples are placed in the degradation chamber with specified environmental conditions for a total of two hours. **b**, RGB images of the samples are taken every 30 seconds for two hours to resolve the time-dependent color change in material. **c**, Computer vision is used to segment each deposited sample over time, $\Phi(t)$, to compute the degradation intensity metric, I_c . This figure reproduced with permission from Siemenn and Aissi *et al.* [8]

3.1 Introduction and Overview

The Archerfish system presents a unique opportunity as a high-throughput synthesis method to explore the perovskite material space, however high-throughput material synthesis without characterization is insufficient to accelerate the rate of materials discovery. In this chapter, I present a high-throughput characterization algorithm to extract the stability of Archerfish produced perovskite samples.

As a lead halide perovskite degrades, it changes color from black to yellow, a result of a phase change and/or decomposition of the structure [10–12]. We leverage this RGB-detectable degradation mechanism [13] and use parallelized computer vision segmentation to automate the detection of degradation within perovskites, as shown in Figure 3.1c. Three sets of Archerfish produced FAPbI₃ to MAPbI₃ gradients, also called samples, totalling $N = 201$ droplets, were degraded for 2 hours in an environmental chamber as shown in Figure 3.1 under 0.5 suns illumination at 34.5°C. The perovskite gradients were synthesized as explained in section 2.4. RGB images of each gradient were taken every 30 seconds as the perovskite droplets degraded. We compute the degradation intensity, I_c , of each perovskite droplet by integrating its change in color, R , over time, t [10]:

$$I_c(\hat{X}, \hat{Y}) = \sum_{R=\{r,g,b\}} \int_0^T |R(t; \hat{X}, \hat{Y}) - R(0; \hat{X}, \hat{Y})| dt, \quad (3.1)$$

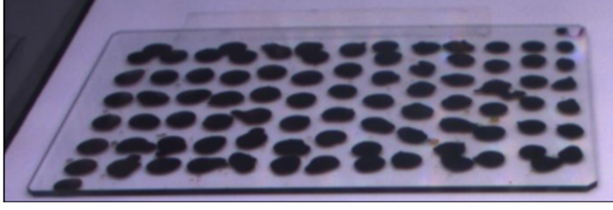
where T is the duration of the degradation and the three reflectance color channels are red, r , green, g , and blue, b , for each sample, $(\hat{X}, \hat{Y})_n \in N$. High I_c indicates high color change, corresponding to high degradation; I_c close to zero indicates low color change and low degradation.

3.2 Detecting Perovskite Degradation from RGB Time Series Data

3.2.1 Segmentation and Identification of Droplets

To start the analysis of the RGB images obtained at each time step of a samples degradation, the first image in the series is chosen and used to identify the location of the droplets within all the RGB images. Because the camera and the substrate do not move, the droplets only need to be identified in one image and these positions are used for all subsequent images in the series. First, the image is cropped to remove most of the background and include only the droplets on the glass substrate. This cropped image is then segmented using a series of morphological operations and the open-cv watershed algorithm.[8] The result is a gray-scale image with each droplet identified and labeled as shown in Figure 3.2. After segmentation the image is eroded and dilated to remove noise and maximum the number of pixels captured for each droplet.

A. Cropped Image



B. Result of the Watershed Segmentation

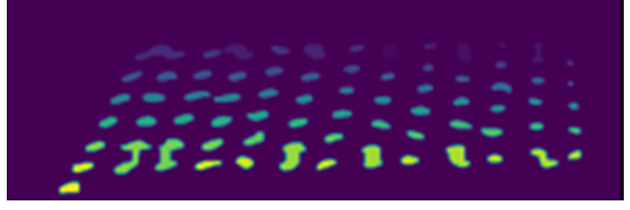


Figure 3.2: a) The droplets on the glass substrate cropped out of the first image in the series. b) Each droplet is identified and labeled as the output of the watershed image segmentation algorithm.

3.2.2 Color Calibration

To use color as a reproducible and repeatable quantitative proxy for degradation, color calibration needs to be applied because the illumination conditions in the environmental chamber may create distortions to the true sample color. At the beginning of the degradation study, an image of a reference color chart (X-Rite Colour Checker Passport; 28 reference color patches), I_R , is taken under the same illumination conditions as the perovskite semiconductor samples. Images at each time step, $\Omega(\Delta t)$, are transformed into CIELAB colorspace and subsequently into a stable reference color space, CIE 1931 color space with a 2-degree standard observer and standard illuminant D50, by applying a 3D-thin plate spline distortion matrix D [10, 14] defined by I_R and known colors of the reference color chart:

$$D = \begin{bmatrix} V \\ O_{4,3} \end{bmatrix} \begin{bmatrix} K & P \\ P^T & O_{4,4} \end{bmatrix}^{-1} \quad (3.2)$$

Here, $O(n, m)$ is an $n \times m$ zero matrix, V is a matrix of the color checker reference colors in the stable reference color space, P is a matrix of the color checker RGB colors obtained from I_R , and K is a distortion matrix between the color checker colors in the reference space and in I_R . The matrix V, K, P , and O are further described in Equation 3.3,

$$\begin{aligned} V &= \begin{bmatrix} 1 & x'_1 & y'_1 & z'_1 \\ \vdots & \vdots & \vdots & \vdots \\ 1 & x'_N & y'_N & z'_N \end{bmatrix}, \\ P &= \begin{bmatrix} 1 & x_1 & y_1 & z_1 \\ \vdots & \vdots & \vdots & \vdots \\ 1 & x_N & y_N & z_N \end{bmatrix}, \\ K &= \begin{bmatrix} 0 & \dots & U(r_{1N}) \\ U(r_{21}) & \dots & U(r_{2N}) \\ \vdots & \vdots & \vdots \\ U(r_{N1}) & \dots & 0 \end{bmatrix}, \end{aligned} \quad (3.3)$$

where $N = 24$ and is the number of colour patches on the X-Rite colour card, and $U(r_{ij})$ is given by:

$$U(r_{ij}) = 2r_{ij}^2 \log(r_{ij} + 10^{-20})$$

$$r_{ij} = \sqrt{(x_i - x_j)^2 + (y_i - y_j)^2 + (z_i - z_j)^2} \quad (3.4)$$

Here, r_{ij} is the Euclidean distance between the CIELAB values of the color patches under the current illumination given by x_i, y_i , and z_i and CIE 1931 color space values of the color patches given by x_j, y_j , and z_j . Vectorization techniques are employed for more efficient calculation of the distortion matrix D . The result of the color calibration algorithm is shown in Figure 3.3 and it observed that the purple hue produced by the illumination condition has been rectified.

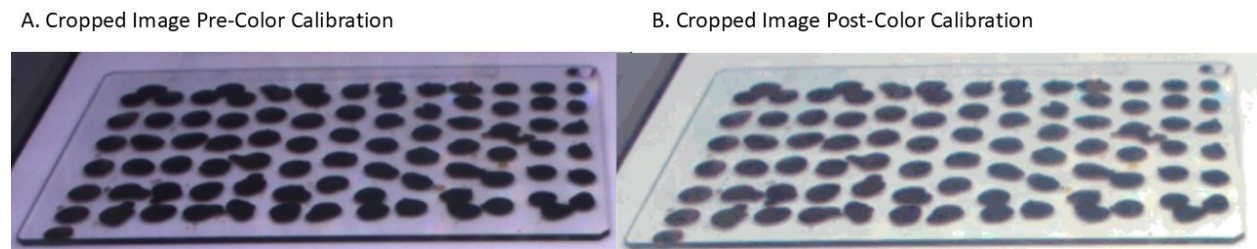


Figure 3.3: a) The cropped image of the perovskite droplets before it is processed by the color-calibration algorithm. b) The same image post calibration, note that the true color of droplets are now accessible and the purple hue created by the illumination conditions have been rectified.

3.2.3 Composition Extraction

After identifying the location of the droplets and performing color calibration, it is necessary to determine estimated values of the droplets composition in order to extract meaningful scientific information. However, due to the positioning of the camera, a perspective change is needed to access the true distance between the droplets and back-propagate their composition using the syringe pump speeds and the travel path of the printer head. [8] The algorithm for this change in perspective consists of two parts: corner detection and warping. Corner detection involves a series of morphological and mathematical operations to detect the four corners of the 2" x 3" glass substrate onto which the droplets are deposited. First the cropped RGB image of the droplets on their substrate is converted to gray-scale and thresholded. Canny edge detection is then performed on the thresholded image to extract its dominant contours. The contour corresponding to droplets are removed using the pixel locations from the segmentation algorithm in Section 3.2.1. A Hough Lines transform is then performed on the remaining contours to determine the dominant lines in the image. For each dominant line, the slope and y-intercept is calculated and used to form a linear equation representation to determine the angles between the lines and their intersection points. These angles and points are used to remove extraneous lines that most likely do not belong to the glass

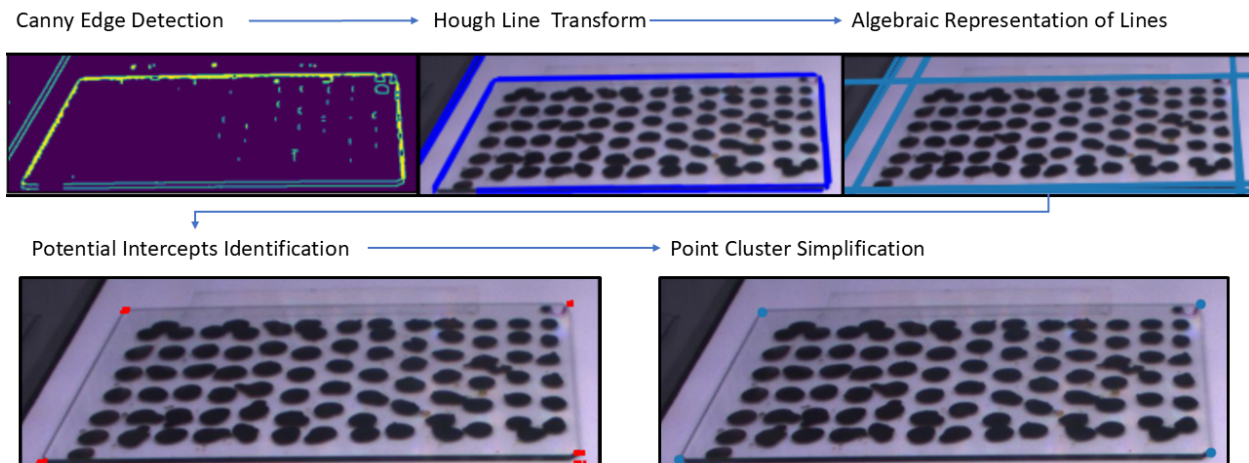


Figure 3.4: The first step in composition extraction is determining the corners of the glass substrate onto which the droplets are printed. This is done through a series of computer vision morphological operations and algebraic representations.

substrate. Lines that have less than 10 degrees between them, for example, are likely to be clusters of lines corresponding to the same edge in the image, they are therefore removed and only one of the lines is kept as a candidate for the edge of the glass substrate. Moreover, because the substrate is a rectangle whose edges intersect within the image, we remove lines that intersect outside the image as they are unlikely to corresponding the the edges of the substrate. Likewise, the intersection points that lie outside the image or along the edges of the image are removed. Finally, clusters of points that emerge near the corners of the substrate can be joined to elucidate the true location of the substrate corners within the image. This is achieved by taking the Euclidean distance between all remaining intersection points and condensing pairs of points into midpoints and repeating this process until all points are sufficiently far from one another. These steps result in the identification of the substrate edges and four corners as shown in Figure 3.4 which are then used to obtained a perspective transform and warp the image into a birds eye view of the droplets as shown in Figure 3.5.

3.2.4 Instability Calculation

Using the color-calibrated images, droplet composition, and droplet pixel locations given by Φ , a final array, $R(t; \hat{X}, \hat{Y})$ of the average color at time t for perovskite semiconductor of composition $\text{FA}_{1-x}\text{MA}_x\text{PbI}_3$ is created. The color of each droplet is measured to determine the stability metric I_c [10], calculated using Equation 3.1. A time series representation of the color of each droplet in a sample is given in Figure 3.6.

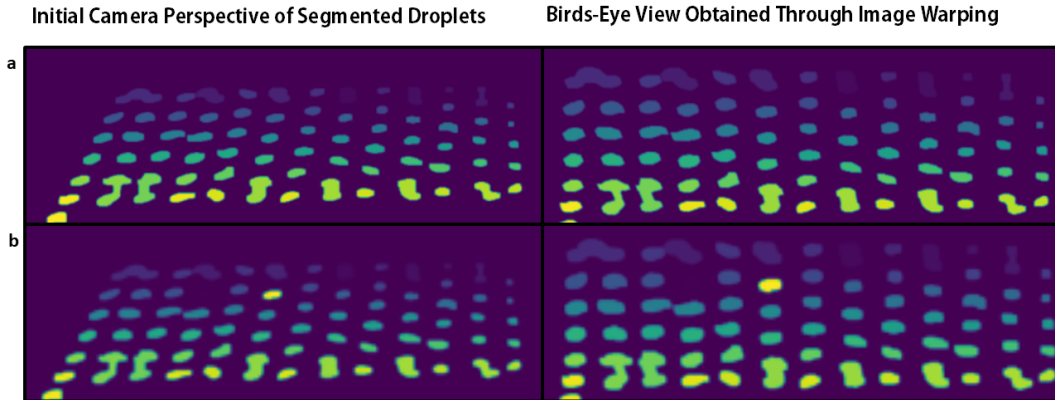


Figure 3.5: The second step in composition extraction is a perspective transform to obtain a bird’s eye view of the droplets. a) This row provides the results of the perspective warp on all the Archerfish droplets. b) In this row, the same droplet is highlighted in yellow to indicating the retention of spatial information for each droplet, the yellow droplet appears in the same position relative to other droplets in both the initial and the warped perspectives.

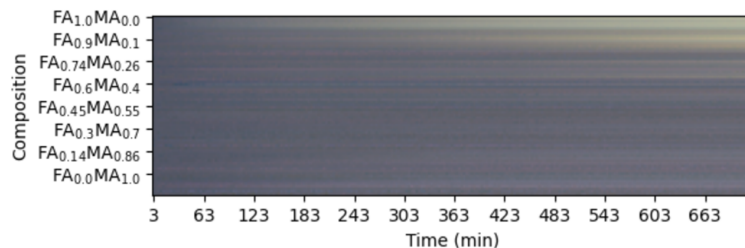


Figure 3.6: An example of a time series color change of every droplet in a sample. Each horizontal line represents the color of a droplet along the $\text{FA}_{1-x}\text{MA}_x\text{PbI}_3$ ($0 \geq x \geq 1$) compositional gradient over the degradation experiment.

3.3 Results

The performance of the degradation autocharacterization is demonstrated by comparing the output I_c to the ground truth degradation, obtained from the pre- and post-band gap deviation [10, 15]. Figure 3.7a illustrates the output of the autocharacterization where high computed I_c values strongly correspond to the occurrence of the ground truth degradation in the samples (yellow scatter points). The determination of ground truth degradation is conducted by a human domain expert. This classification performance of the autocharacterization algorithm achieves a maximal accuracy of 96.9%, relative to the ground truth. The yellowing pattern of the FA-rich samples is shown in Figure 3.7b as a result of the phase change from favorable cubic phase α -FAPbI₃ to the non-perovskite hexagonal phase δ -FAPbI₃ [11]. Furthermore, running a full degradation detection computation using autocharacterization takes only 20 minutes per 200 samples, given 48000 total degradation images over the 2-hour degradation experiment. This is a significant speedup from the stan-

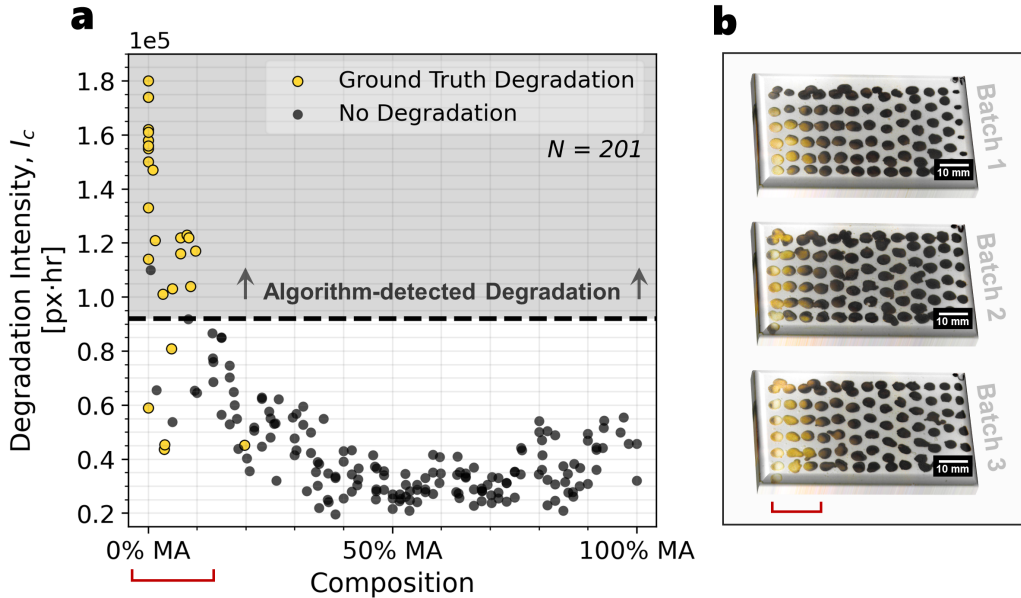


Figure 3.7: **a**, Performance of the autocharacterization of degradation intensity, I_c , relative to the ground truth degradation determined by a domain expert (yellow scatter points) on $N = 201$ unique perovskite samples across 3 independent trials. The black dashed line indicates the split between high and low I_c values, corresponding to high and low degrees of degradation, respectively. **b**, Images of the three batches of $\text{FA}_{1-x}\text{MA}_x\text{PbI}_3$ gradient samples after the 2-hour controlled degradation. The leftmost samples are FA-rich and the rightmost samples are MA-rich. The yellowed FA-rich compounds have undergone a phase transition from $\alpha\text{-FAPbI}_3$ to $\delta\text{-FAPbI}_3$ and are considered as “ground truth” degradation samples if they exhibit a deviation of $> 0.02\text{eV}$ in band gap from pre- to post-degradation, evaluated by a domain expert. This figure reproduced with permission from Siemenn and Aissi *et al.* [8]

dard microscopy or XRD methods of determining degradation, which can take hours or days to identify the degradation of an equivalent number of samples.

Using the fast and accurate stability autocharacterization tool developed in this thesis, we tractably generate an ultra-high resolution stability trend for the $\text{FA}_{1-x}\text{MA}_x\text{PbI}_3$ series, shown in Figure 3.7a and this trend has not been reported at such a high resolution yet in literature. Prior literature reports stability compositional resolutions from $0 \leq x \leq 1$ for 11 compositions [16], 9 compositions [17], and 7 compositions [18] using conventional characterization methods. Moreover, Charles *et al.* [16] reports the stability at $x \approx 0.1$ compositional increments from $0 \leq x \leq 1$ using 6 time steps, amounting to a total of 66 temporal data points. Comparatively, using automated characterization, we report the stability at $x \approx 0.008$ unique compositional increments from $0 \leq x \leq 1$ using 240 time steps, amounting to 28800 unique temporal data points (with 48000 total temporal data points). Thus, with autocharacterization, we achieve over a 10x increase in the compositional resolution and a 40x increase in the temporal resolution for a total of a 436x increase in the number of unique data points reported for the $\text{FA}_{1-x}\text{MA}_x\text{PbI}_3$ stability series, to our

knowledge.

Furthermore, with this high-resolution stability trend, we note the same regions of high-degradation appear in Figure 3.7a as do in the literature for the α -FAPbI₃ \rightarrow δ -FAPbI₃ degradation pathway at $0.0 \leq x \leq 0.15$, with the optimal low-degradation region occurring at $x \approx 0.40$ [16, 19].

Through the generation of ultra-high resolution trends, we may achieve a better understanding of complex semiconductor composition-property relationships to enable higher-performance design of materials in the future.

3.4 Chapter Summary

In this chapter, I provided a study that successfully combines high-throughput synthesis and characterization methods to speed up the rate of information gathering about a material system. Gradients of FA_{1-x}MA_xPbI₃ ($0 \leq x \leq 1$) perovskite solar cell materials with N=201 droplets were synthesized using the improved version of the Archerfish system described in Chapter 2 and characterized using computer vision image processing algorithms to extract their stability, a key material property for perovskites.

Chapter 4

Limitations of the Platform

4.1 Introduction and Overview

The architecture presented for high-throughput combinatorial printing with Archerfish is promising and has been used to print gradients of several different material systems [8]. However, with its current design, Archerfish can only print gradients, not specific compositions, and has many limitations that can result in poor reliability and reproducibility of samples. These limitations can be categorized into three main categories: compositional control, droplet generation, and environmental and crystallization control. Each category has unique limitation considerations for the current tool but also invites opportunities for growth and design.

4.2 Lack of Compositional Control

Compositional control refers to the ability to set and determine the compositions of individual droplets. With Archerfish's current architecture, it is not possible to set a specific composition for each droplet or determine a droplet's exact composition without additional measurements, such as Energy-dispersive X-ray spectroscopy (EDS). This limits Archerfish to printing gradients with known endpoints that are pre-loaded as precursors in the syringes. Compositional control is limited by various factors but major contributors such as pressure build-ups and fluid reservoirs have been identified and are further discussed here.

Pressure build-ups in areas of compliance within the fluid lines create non-linearities in flow rates. For example, the syringes use a silicone rubber plunger and as a result, fluid is not always dispensed when the motors push the plunger, instead, the plunger compresses to accommodate the resulting pressure from the positive displacement as shown in Figure 4.3. Discontinuities in expected flow rates are also linked to the pressure build-up in the compliant plunger or fluid lines. Another main hindrance to compositional control is the presence of fluid reservoirs that result in hard-to-predict mixing behavior, which ultimately average out to produce a gradient, but do not seem to be linear at each time step. Reservoirs within the valve generate vortices and can result in residual contamination that complicates the transition between fluids, producing unknown compositions at the output droplet. To reduce cross-contamination between runs, reservoirs must also be purged. These purging

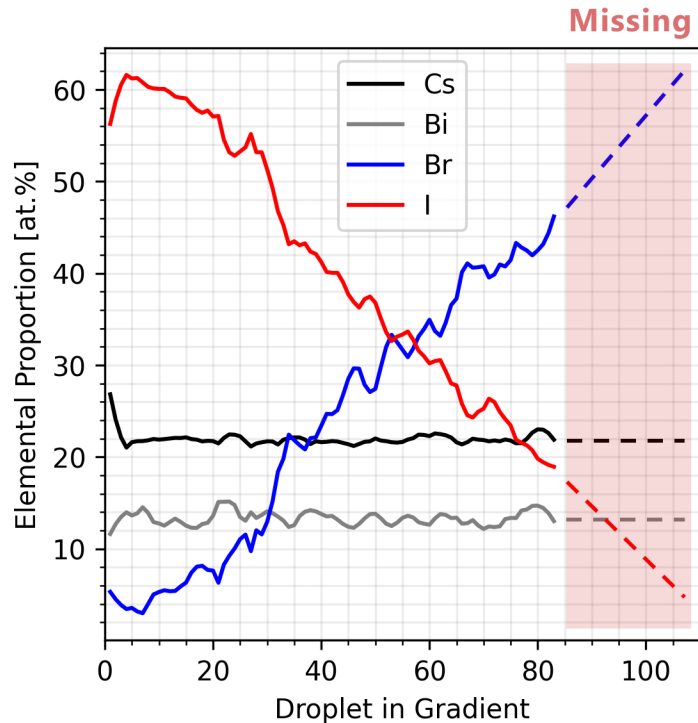


Figure 4.1: Energy-dispersive X-ray spectroscopy (EDS) elemental composition traces. These elemental traces are shown for a $\text{Cs}_3\text{Bi}_2\text{I}_9$ - $\text{Cs}_3\text{Bi}_2\text{Br}_9$ (cesium bismuth iodide-cesium bismuth bromide) perovskite gradient printed using Archerfish where each droplet has its EDS spectrum measured. We note the abrupt stop in the compositional shift between iodine and bromine due to improper tuning of the Archerfish print settings. Approximately 80% of the entire gradient is shown to be successfully printed here, the missing portion of the gradient is visualized using dashed line projections. This figure reproduced with permission from Siemenn and Das *et al.* [20]

steps take much longer than the prints themselves, sometimes up to a minute, and waste precursors. Fluid inertia can also pose a problem as pulses in the syringe pump can lead to large volumes of liquid being dispensed periodically, adding more deviation to the expected flow rate. Due to the step-wise rotation of the stepper motors, the syringe pumps create oscillations in the fluid flow, as shown in Figure 4.2 that do not affect the overall gradient composition but could impact the composition of individual droplets. Over-pressurization and back-flow in the fluid lines further limit compositional control and create leaks in the system. Differences in flow rates and thus fluid pressure can at times lead to back-flow and cross contamination between fluid lines, with one fluid forcing its way into another syringe instead of exiting through the nozzle. This behavior is aided by compliant materials in the fluid path that expand to allow build-ups of fluid. This problem could be resolved by the use of check-valves in the flow path thereby forcing the fluid to exit through the nozzle. Lastly, important questions regarding the impacts of pressure, fluid viscosity, temperature, and other parameters on fluid composition and deposition require further analysis and study.

These questions have not yet been explored, but are critical to precise compositional control.

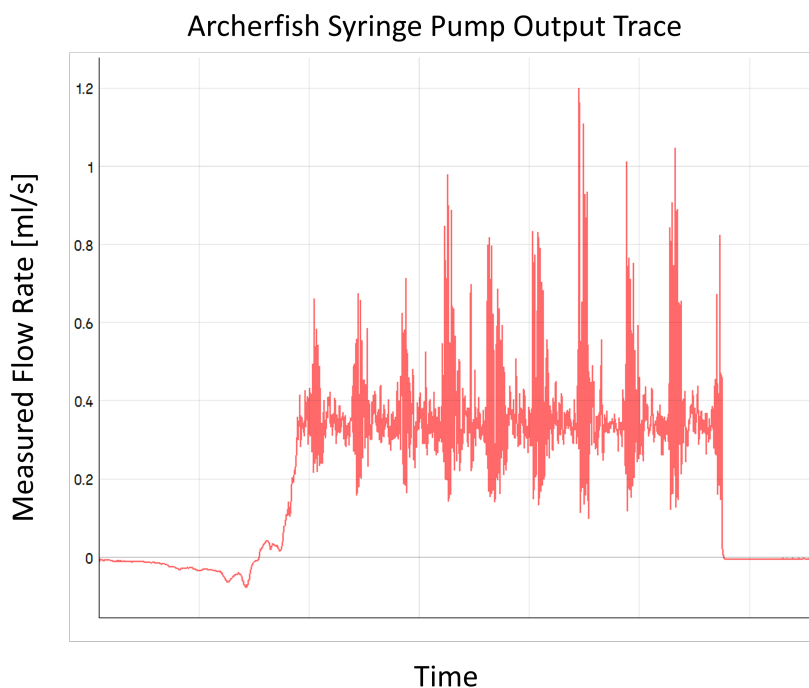


Figure 4.2: The measured flow rate from the current \$10 Archerfish syringes with a constant motor speed. Large and small oscillatory spikes with magnitudes of up to 333% of the set flow rate occur periodically due to the rotation of the stepper motor. The x-axis is in 20 second intervals.

The lack of compositional control reduces the reliability of Archerfish and makes it more difficult for researchers to use the system. For example, it took three researchers two days to find the right parameters to create an end-to-end gradient for the FAPbI_3 - MAPbI_3 perovskite series due to the complex relationship between the droplet wetting properties, reservoirs, compliant regions, and standing waves within the fluid lines. Figure 4.1 illustrates the EDS-measured elemental traces of an 80-droplet $\text{Cs}_3\text{Bi}_2\text{I}_9$ - $\text{Cs}_3\text{Bi}_2\text{Br}_9$ (cesium bismuth iodide-cesium bismuth bromide) perovskite series printed with Archerfish that did not have its printing parameters properly tuned. This improper tuning resulted in approximately only 80% of the entire gradient being printed, stopping before reaching the $\text{Cs}_3\text{Bi}_2\text{Br}_9$ end point.

4.3 Droplet Generation

Archerfish can deposit gradients of uniformly thick droplets on most prints but this uniformity can vary based on the precursor molarity and properties of the fluid or substrate. Substrates with higher wettability often distort the droplets, limit droplet packing, and add variability to their shape. It has been observed that wetting behavior can even change between prints of the same materials on the same substrate. Moreover, the relationship between droplet shape and the PWM driver has not been characterized in detail, making it

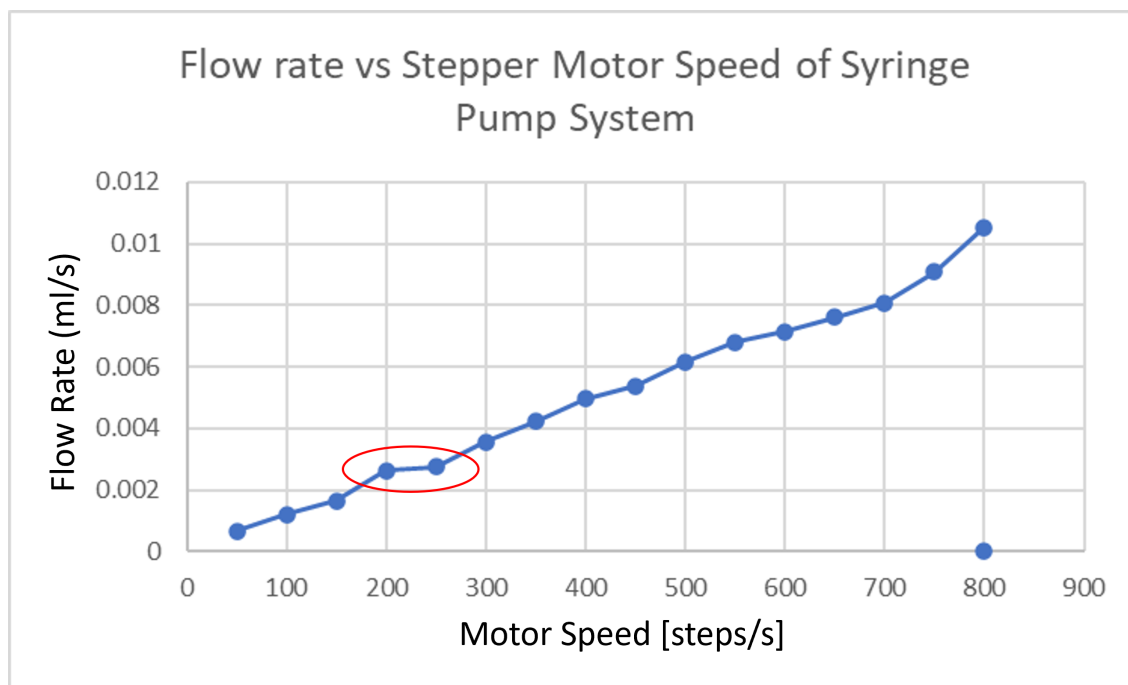


Figure 4.3: Results of a flow rate measurement test indicates non-linearities in the expected flow rate due to a pressure build-up effect. The syringe was refilled between the data points circled in red, despite an increase in the motor speed, the flow rate after a refill remains nearly the same. This effect is a result the rubber plunger in the syringe relaxing when drawing in fluid and therefore needing to re-pressurize before any fluid is dispensed.

difficult to change the droplet generation parameters along with the gradient parameters in accordance with the substrate wettability.

Archerfish droplets with low molarity are subject to the coffee ring effect, in which higher evaporation rates at the droplet's edge cause radial migration of the species in the fluid. This phenomenon produces a droplet with a thicker outer ring of high species concentration and a thinner inner area of low species concentration [21]. Figure 4.4 illustrates these differences in species migration rates for a low molarity Archerfish droplet. For most material systems, the downstream characterization effects of this coffee ring can be avoided through post-processing techniques and focusing characterization on only the uniform inner area of the droplet. Satellite droplets can also form during the droplet deposition process, which do not hinder characterization but are, nonetheless, undesirable.

4.4 Environmental and Crystallization Control

Environmental and crystallization control refers to the ability to control and create uniform crystallization conditions across all droplets on an Archerfish print. Crystallization control is not necessary for all Archerfish samples, however, some material systems cannot be studied without it. Since Archerfish is designed to be a general experimental tool, no aspect of the device is devoted to post-processing any one specific material system. For example,

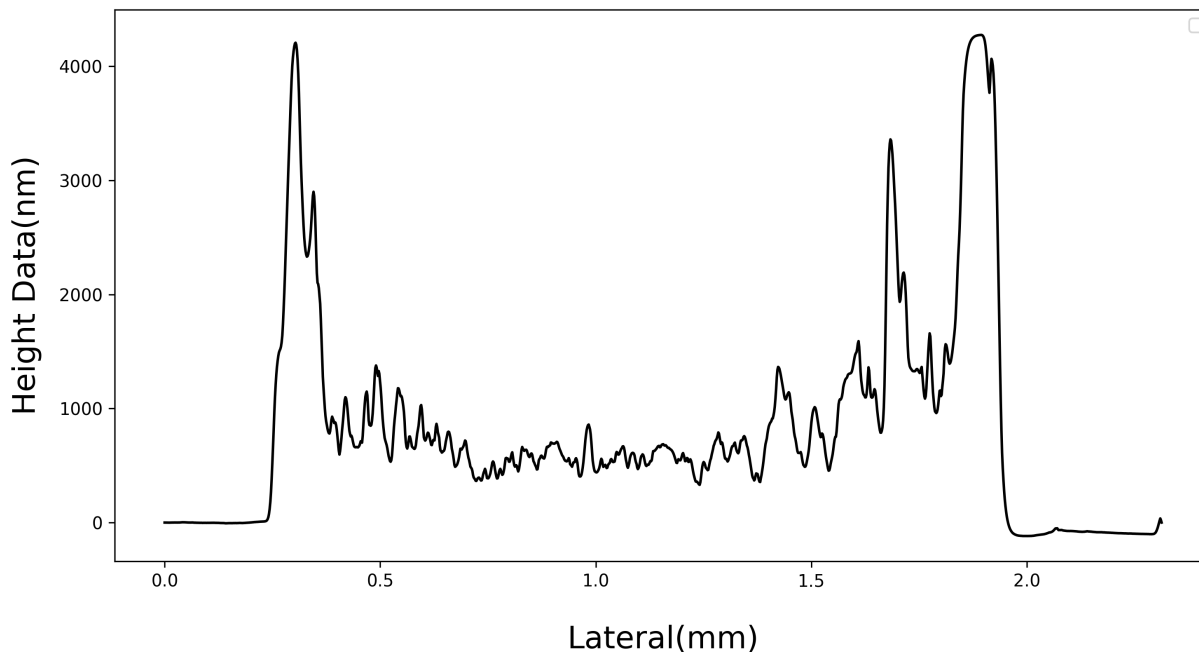
Thickness Profile of a $Cs_3Bi_2Br_9 - Cs_3Sb_2I_9$ Perovskite Droplet

Figure 4.4: The profile of a droplet along the $Cs_3Bi_2Br_9$ to $Cs_3Sb_2I_9$ perovskite gradient obtained through stylus profilometry. A coffee ring effect can be seen, with high ridges along the edge of the droplet and a near-flat film in the middle.

Archerfish does not maintain a constant temperature, pressure, or humidity around samples while or after they are printed, as these conditions would vary across different material systems.

This lack of environmental control presented a challenge for the synthesis of perovskite gradients, limiting our ability to study crystallization-dependent properties like stability. Inconsistent degradation patterns across Archerfish prints arose due to the non-uniform crystallization of droplets. Figure 4.5 shows the controlled degradation of two perovskite samples of the same $FAPbI_3$ - $MAPbI_3$ compositional gradient. Varying degradation patterns were observed due to non-uniformities in droplet geometry and hot plate surfaces during annealing. While not in the original scope of the project, future versions of Archerfish should include tunable environmental control to expand the material systems that can be synthesized and studied.

4.5 Unknown Mixing Mechanisms

Due to the small pipe diameters and low flow rates, the Archerfish fluid streams operate in the laminar flow regime making it nearly impossible for passive mixing to occur at the length scales of the fluid lines after the junction. The flow regime can be identified via the value of the Reynolds number which is defined as:

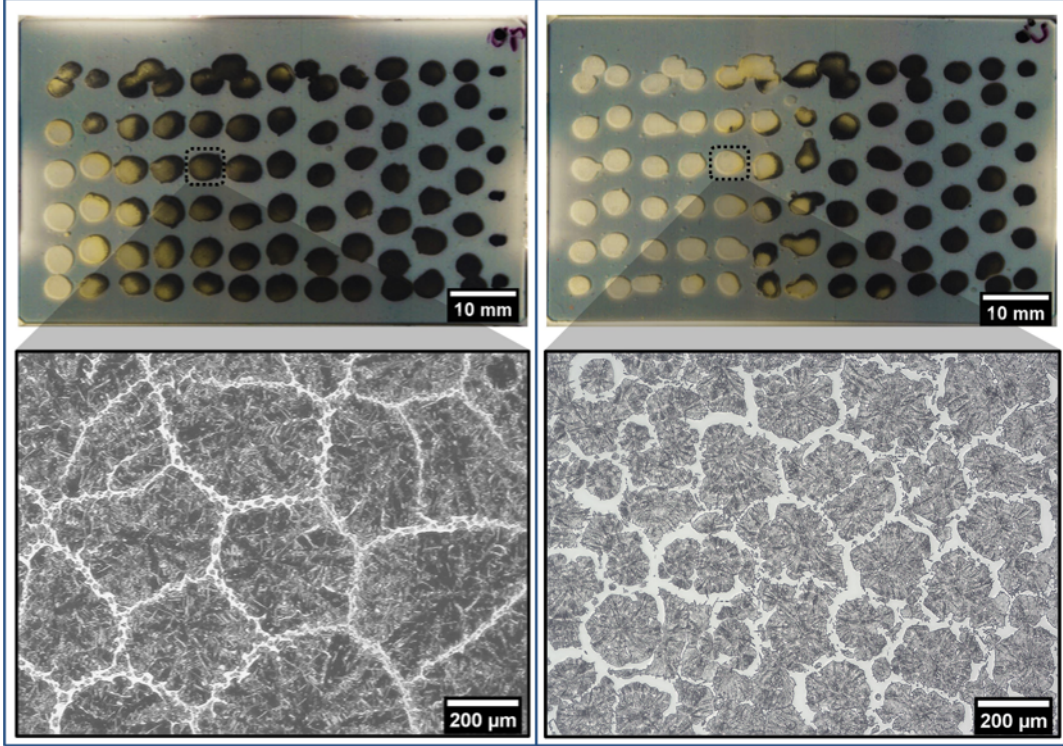


Figure 4.5: Two different Archerfish prints of the same $\text{FAPbI}_3\text{-MAPbI}_3$ compositional gradient after annealing and controlled degradation. Yellow samples are degraded while black samples are not degraded. These two perovskite gradients exhibit different degradation patterns despite being of the same composition and degrading under the same conditions. The differences in crystallization, as shown by the SEM images, transpired from spatial non-uniformities in the annealing and deposition processes. This figure reproduced with permission from Siemenn and Das *et al.* [20]

$$Re = \frac{\rho u L}{\mu} \quad (4.1)$$

where ρ is the fluid density, u is the fluid velocity, L is the pipe diameter, and μ is the dynamic viscosity of the fluid. Passive mixing can be expected in turbulent flow regimes characterized by Reynolds numbers above 2,000. For Archerfish operating with near 1 centipoise fluids, the Reynolds number ranges from 0.3 to 30. Figure 4.6 provide optical microscope images of a 4-way junction machined from acrylic for visual inspection of the Archerfish junction. Laminar flow with no mixing is observed, as expected due to the low Reynolds numbers of this system. However, optical microscopy images from before and after the old Archerfish system's Lee valve indicate that mixing could potentially be achieved by agitation from a valve as shown in Figure 4.7. Precursor flows with higher viscosity or lower Reynolds numbers could require more folds or obstacles within the plumbing lines to promote more uniform mixing.

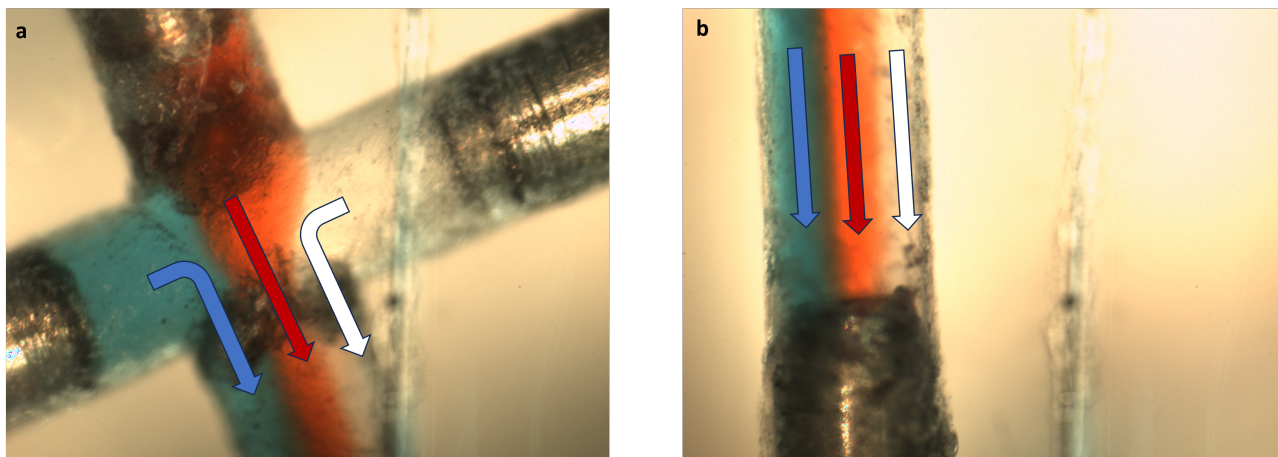


Figure 4.6: Optical microscope images through a machined acrylic 4-way junction with 1/32” inner diameters fluid paths of a) the point of fluid stream contact with clear separation and no mixing and b) the inlet to the droplet generator indicating, as expected, that no mixing occurs when the fluid streams meet. The arrows indicate the direction of flow.

4.6 Other Limitations

Beyond the concerns presented by a lack of compositional control, droplet generation, and environmental and crystallization control, several minor but impactful limitations warrant a mention.

4.6.1 Material Compatibility

The current wetted materials in the Archerfish plumbing lines are PTFE, silicone, and polypropylene. While PTFE is resistant to a wide range of chemicals, silicone and polypropylene are not, which limits the materials that can be studied with the current Archerfish design. Future iterations of the designs should therefore include a carefully chosen material path with highly chemically resistant tubing and actuators.

4.6.2 Human Introduced Variation

Full integration of each Archerfish subsystem is lacking. The retrofitted 3D printer and the actuators (pinch valve and microcontroller) are independently controlled. The pi data center controls the syringe pumps and valve, however the 3D printer gantry is not yet integrated into the central data center. There is no connection between the deposition location and the droplet generation leading to variation between prints, even with the same operator, as the 3D printer and droplet generators may not always be activated simultaneously. Human to human variation is also introduced between prints as the two sub-systems cannot be activated simultaneously and in the same order by every operator. One operator may choose to start the pinch valve before the 3D printer, and another may do the opposite.

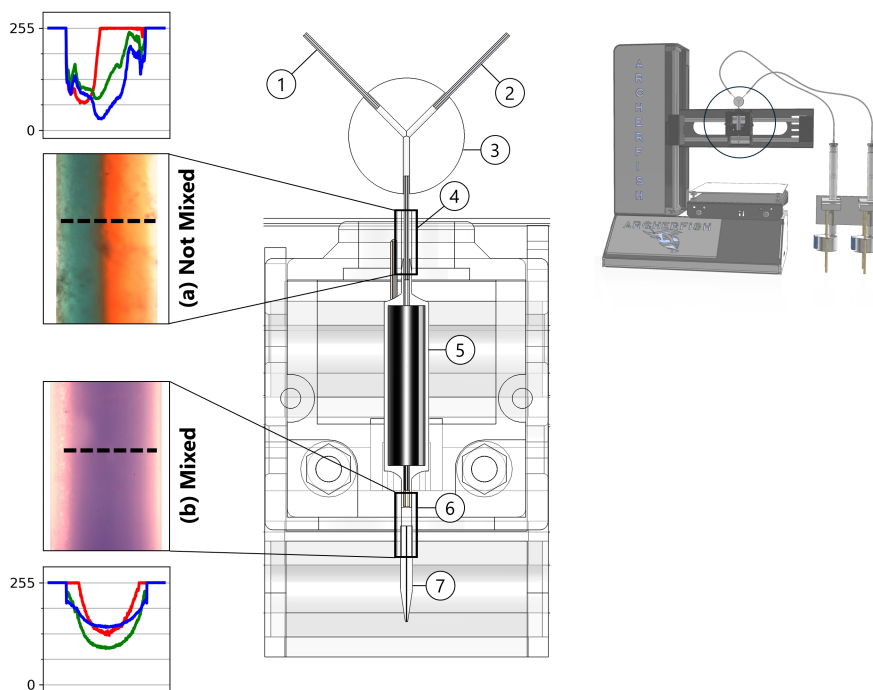


Figure 4.7: Optical microscope images through a machined acrylic three-way junction with inlets at 90 degrees. RGB color analysis show mixing at the outlet of the old Archerfish Lee valve, suggested that agitation via the valve could be a viable path to achieve known mixing for Archerfish droplets. Figure reproduced with permission from Siemenn and Das *et al.* [20]

4.6.3 Lack of System Feedback

Human to human variations can be further exacerbated by the lack of real-time data acquisition during the printing procedure. Currently, there are no monitoring sensors in the fluid path or on the actuators, there is therefore no way to measure what the system is outputting. The syringe pumps for example, have shown discontinuities in flow rates but these discontinuities currently are not being measured. For example, an encoder on the stepper motors could provide insight on the true flow rate output of the syringe pumps, and time logs indicating when each subsystem is activated could help predict and explain variations between prints.

4.7 Chapter Summary

In this chapter, I present a thorough discussion of limitations and failure modes of the Archerfish system. These include: lack of compositional control, poor environmental control, droplet morphological instabilities, and unknown mixing behavior amongst others. In the next chapter I will provide a conclusion, with a summary and future work for the methods developed throughout this thesis.

Chapter 5

Conclusion

5.1 Summary

In this thesis I presented a high-throughput workflow for synthesizing and characterizing perovskite materials. I introduced the Archerfish system as developed by Siemenn *et al.* [2], explained its limitations, and described several improvements that I implemented to allow it to be used with perovskite materials. I presented XRD, XPS, and hyper-spectral imaging results that validated the improved systems ability to synthesis perovskite crystalline materials. I then demonstrated a high-throughput characterization algorithm to extract the stability of 201 perovskite droplets generated through the Archerfish platform. Lastly, I discussed the limitations of the platform and opportunities for future improvements.

5.2 Future Work

The work discussed in this thesis provides an example of low-cost but high-throughput automated research tools that can decrease synthesis time and increase productivity for small labs. The Archerfish platform as presented has a lot of potential, however as discussed in Chapter 4.1, there are several limitations that still require further development before it can be launched as tool for research. Future work includes further improvements to the Archerfish system specifically focused on mixing, more robust fluid lines and connections, and better communication protocols to join all components of the system under one central command center.

Appendix A

Archerfish Components List

Summary Table				
Description	Cost	Supplier	Part	Qty
Solenoid pinch valve; 2-way NO, 1/32" ID x 3/32" OD, 12/24V	\$108.00	Precigenome		1
Monoprice MP Select Mini 3D Printer (discontinued)	\$175.99	Mono Price		1
300 um Diameter Flow-focusing micro-nozzle outlet	\$50.00	Small Precision Tools	1551-120-437P 200 (10-11D-20)	1
Arduino Mega	\$48.90	Amazon	B0046AMGW0	1
ZK-PP2K 24V High Power PWM Driver	\$10.57	Amazon	B0C7H1QFR8	1
24V Variable Power Supply	\$45.99	Amazon	B08GFSVHLS	2
Raspberry PI 3 Model B+	\$44.41	Amazon	B0BNJPL4MW	1
Raspberry Pi Touch Screen Monitor	\$32.99	Amazon	B07RZYYNMZ	1
Bluetooth KeyBoard and Mouse	\$19.79	Amazon	B07WV5WN7B	1
28BYJ-48 DC 5V Stepper Motors + ULN2003	\$7.99	Amazon	B0CLYCM1CP	1
Fittings, Tubing, and Pumps	\$23.39	Home-Built + McMasterCarr		
Total	\$568.02			

Table A.1: General component list for the improved Archerfish system. Detailed bill of materials and building instructions for version one of the Archerfish Platform are provided by Siemenn *et al.* [20]

Appendix B

Archerfish Raspberry Pi Code

```
1 # import needed libraries
2
3
4 import PySimpleGUI as sg
5 import serial
6 import time
7 import numpy as np
8 from datetime import datetime
9
10 serialcomm = serial.Serial('COM4', 9600)
11 serialcomm.timeout = 1
12
13
14 # Save Experiment Setup Data in text file
15
16
17 def save_data(precursors, relative_speeds, mode):
18     # saves precursor and relative speed data
19     # may need to change to accommodate gradient type experiments
20     now = datetime.now()
21     f = open('Experimental_log.txt', 'a')
22     # Input Date and Time then table of precursors and speeds for
23     # this specific experiment
24     # P1 P2 ....
25     # S1 S2 ....
26
27     t_string = now.strftime("%H:%M:%S")
28     d_string = now.strftime("%B %d, %Y")
29     dt_string = d_string + ' ' + t_string + '\n'
30     f.write(" \n")
31     f.write(" ----- \n")
32     f.write(f"New {mode[0]} Experiment \n")
33     f.write(dt_string)
```

```

33     f.write(f"Precursors are:      {precursors} \n")
34     if mode == ['Batch']:
35         f.write(f'Relative Speeds are: {relative_speeds} \n')
36     else:
37         f.write(f'Steps, Percent of 3rd Precursor, and Gradient Range
38                 are: {relative_speeds} \n')
39     f.close()
40
41 # Set Up Window Layout
42
43
44 def setup_window(def_mot, max_precursor_number):
45     choose = ['Batch', 'Two Fluid Gradient', 'Constant + Two Fluid
46              Gradient']
47     layout = [[sg.Text("Choose Experiment Type", justification="c")],
48              [sg.Listbox(choose, size=(30, len(choose)), key='-EXP
49              -'),
50              [sg.T("Number of Precursors: ", justification="r"),
51              sg.I(key="-IN-")],
52              [sg.Button("Ok")]]
53
54     window_title = "ArcherFish Command Center"
55     window = sg.Window(window_title, layout)
56
57     while True:
58         event, values = window.read()
59         # cont = ''
60         if event == sg.WINDOW_CLOSED:
61             break
62         if event == "Ok":
63             # Output the set-up choices
64             # Put in error messages in case they forget to put a
65             # number
66             # of motors or don't choose an experiment
67             if not values['-EXP-']:
68                 sg.popup_error("You must choose a mode", modal=True)
69             if values['-EXP-']:
70                 choice = values['-EXP-']
71                 mot = values['-IN-']
72                 if choice == ['Batch']:
73                     if len(mot) == 0:
74                         mot = str(def_mot)
75                 elif choice == ['Two Fluid Gradient']:
76                     mot = str(2)
77                 cont1 = sg.popup_ok_cancel("For Two Fluid
78                 Gradient mode you must use two precursors.",

```

```

modal=True)
74     if not cont1 == 'OK':
75         window.close()
76         return choice, int(mot), cont1, int(
            max_precursor_number)
77     elif choice == ['Constant + Two Fluid Gradient']:
78         mot = str(3)
79         cont2 = sg.popup_ok_cancel("For Constant + Two
            Fluid Gradient mode you must use three
            precursors.", modal=True)
80         if not cont2 == 'OK':
81             window.close()
82             return choice, int(mot), cont2, int(
                max_precursor_number)
83     if int(mot) > int(max_precursor_number):
84         sg.popup_error("Maximum number of precursors is
            3, enter a number lower than or equal to 3.")
85     else:
86         cont = sg.popup_ok_cancel(
87             f"Opening command window for {choice[0]}
            experiment with {mot[0]} precursors.",
            modal=True)
88         if cont == 'OK':
89             window.close()
90             return choice, int(mot), cont, int(
                max_precursor_number)
91         else:
92             window.close()
93             return choice, int(mot), cont, int(
                max_precursor_number)
94     window.close()
95
96
97 def batch_window(mots, def_mots, max_precur_num, max_speed,
mode_input):
98     print(mode_input)
99     mode_str = str(mode_input)
100    mode_str = mode_str[:-1]
101    mode_str = mode_str[:-1]
102    mode_str = mode_str[1:]
103    mode_str = mode_str[1:]
104    mode = [mode_str]
105
106    print(mode)
107    mots = int(mots)
108    max_precur_num = int(max_precur_num)
109    max_speed = int(max_speed)

```

```

110 refills = []
111 stopping = []
112 chemicals = ['MAPbI3', 'FAPbI3', 'CsPbI3', 'DMF', 'DMSO']
113 info = ['Gradient Steps', 'Max Percent of Gradient Composition',
114         'Percent of 3rd Precursor']
114 layout = [[sg.T('Set Experiment Parameters')],
115            [sg.HSeparator()]]
116 if mode == ['Batch']:
117     mode_num = 1
118     for i in range(mots):
119         istr = str(i)
120         layout = layout + [[sg.T(f"Precursor {istr[0]} Name:"),
121                             sg.Combo(chemicals, size=(20, 1), key
122                                     =f"-P{istr[0]}-"),
123                             sg.T(f"Precursor {istr[0]} Speed:"),
124                             sg.I(key=f"-S{istr[0]}-")]
124     layout = layout + [[sg.T('')],
125                        [sg.T("Refill Precursors Before You Start
126                               :")],
127                        [sg.HSeparator()]]
127 elif mode == ['Two Fluid Gradient'] or mode == ['Constant + Two
128 Fluid Gradient']:
128     mode_num = 2
129     for i in range(mots):
130         istr = str(i)
131         if i == 2:
132             layout = layout + [[sg.T(f"Constant Precursor Name:")
133                                 ,
134                                 sg.Combo(chemicals, size=(20, 1),
135                                         key=f"-P{istr[0]}-"), sg.Push
136                                 (),
137                                 sg.T(info[i]),
138                                 sg.I(key=f"-S{istr[0]}-", size
139                                     =(20, 1))]
136         else:
137             layout = layout + [[sg.T(f"Precursor {istr[0]} Name
138                                     :"),
139                                 sg.Combo(chemicals, size=(20, 1),
140                                         key=f"-P{istr[0]}-"), sg.Push
141                                 (),
142                                 sg.T(info[i]),
143                                 sg.I(key=f"-S{istr[0]}-", size
144                                     =(20, 1))]
141
142 layout = layout + [[sg.T('')],
143                    [sg.T("Refill Precursors Before You Start
144                           :")],

```

```

144         [sg.HSeparator()]]
145 # print(layout)
146 for j in range(mots):
147     jstr = str(j)
148     if j == 0:
149         layout_left = [[sg.Button(f"Fill Precursor {jstr[0]}")]
150         flush = [f"Flush Precursor {jstr[0]}"]
151         layout_right = [[sg.Button(f"Flush Precursor {jstr[0]}")
152         ]]
153         refills = refills + [f"Fill Precursor {jstr[0]}"]
154         stopping = stopping + ['0000']
155     else:
156         layout_left = layout_left + [[sg.Button(f"Fill Precursor
157         {jstr[0]}")]
158         layout_right = layout_right + [[sg.Button(f"Flush
159         Precursor {jstr[0]}")]
160         refills = refills + [f"Fill Precursor {jstr[0]}"]
161         flush = flush + [f"Flush Precursor {jstr[0]}"]
162         stopping = stopping + ['0000']
163 for f in range (int(max_precur_num) - int(mots)):
164     stopping = stopping + ['0000']
165 layout_left = layout_left + [[sg.Button("Fill All Precursors")]]
166 layout_right = layout_right + [[sg.Button("Flush All Precursors")
167     ]]
168 refills = refills + ["Fill All Precursors"]
169 flush = flush + ["Flush All Precursors"]
170 layout_stop = [[sg.Button("Stop")], [sg.Button("Turn on Valve")]]
171 layout_columns = [[sg.Column(layout_left),sg.VSeparator(),
172     sg.Column(layout_right), sg.VSeparator(), sg.Column(
173     layout_stop)]]
174
175 layout = layout + layout_columns + [[sg.T('')],
176     [sg.T('Make Sure to Recalibrate the Syringes
177     After a Refill')],
178     [sg.HSeparator()],
179     [sg.Button("Recalibrate Syringes",
180         button_color='purple', size=(30, 2))],
181     [sg.Button('Move to Glove Box', button_color='
182     green'), sg.Button('Return to Setup Window'
183     ,

```

```

175
176 window_title = f"{mode[0]} Experiment Command Center"
177 window = sg.Window(window_title, layout)
178 op = bool
179 speeds = []
180 precur = []
181 while True:
182     event, values = window.read()
183     if event == sg.WINDOW_CLOSED:
184         break
185     if event == "Turn on Valve":
186         i = str(1) + str(stopping) + str(1)
187         while True:
188             serialcomm.write(i.encode())
189             time.sleep(0.5)
190             break
191     if event == 'Stop':
192         stopping_str = str(stopping)
193         i = str(1) + stopping_str + '0'
194         while True:
195             serialcomm.write(i.encode())
196             time.sleep(0.5)
197             break
198     if event == "Recalibrate Syringes":
199         i = []
200         for k in range(mots):
201             i = i + ['-050']
202         if mots < max_precur_num:
203             for l in range(max_precur_num - mots):
204                 i = i + ['0000']
205         i = str(1) + str(i) + str(1)
206         while True:
207             serialcomm.write(i.encode())
208             time.sleep(0.5)
209             break
210         time.sleep(20)
211         i = str(1) + str(stopping) + str(0)
212         while True:
213             serialcomm.write(i.encode())
214             time.sleep(0.5)
215             break
216
217     if event in refills:
218         # print(event)
219         i = []
220         if event == "Fill All Precursors":

```

```

221         for k in range(mots):
222             i = i + ['0600']
223     else:
224         wvent = str(event)
225         for k in range(mots):
226             if k == int(wvent[15]):
227                 # building the serial message as ['####', '
                #####', '####']0
228                 # if you are at the location within the
                message for the motor you want to
                communicate with
229                 # make the speed 500, else make the speed 0
230                 i = i + ['0600']
231                 # print(k)
232             else:
233                 i = i + ['0000']
234     for kl in range(max_precur_num - mots):
235         i = i + ['0000']
236     i = str(i)
237     i = str(1) + i + str(0)
238     # print(i)
239     # print(wvent[15])
240     while True:
241         serialcomm.write(i.encode())
242         time.sleep(0.5)
243         break
244     if event in flush:
245         # print(event)
246         i = []
247         if event == "Flush All Precursors":
248             for k in range(mots):
249                 i = i + ['-200']
250         else:
251             wvent = str(event)
252             for k in range(mots):
253                 if k == int(wvent[16]):
254                     # building the serial message as ['####', '
                    #####', '####']0
255                     # if you are at the location within the
                    message for the motor you want to
                    communicate with
256                     # make the speed 500, else make the speed 0
257                     i = i + ['-600']
258                     # print(k)
259                 else:
260                     i = i + ['0000']
261     for f in range(max_precur_num - mots):

```

```

262         i = i + ['0000']
263     i = str(i)
264     i = str(1) + i + str(1)
265     # print(i)
266     # print(wvent[15])
267     while True:
268         serialcomm.write(i.encode())
269         time.sleep(0.5)
270         break
271
272     if event == 'Return to Setup Window':
273         op = False
274         speeds = []
275         precur = []
276         break
277     if event == 'Move to Glove Box':
278         max_speed = int(max_speed)
279         if mode == ['Batch']:
280             op = True
281             # create speeds list which just grabs the exact
282             # values inputted for precursor speeds
283             # Speed values must be between 0 and 1, must sum to
284             # greater than 0.9 but not more than 1 ideally
285             # create list of precursors used
286             for k in range(mots):
287                 kstr = str(k)
288                 speeds = speeds + [values[f"-S{kstr[0]}-"]]
289                 precur = precur + [values[f"-P{kstr[0]}-"]]
290             # print(speeds)
291             # Send Confirmation Message with Precursor and Speed
292             # Values
293             ok_cancel = sg.popup_ok_cancel("You set up an
294             experiment for " + str(precur) +
295             " at the respective
296             speeds of " + str(
297             speeds))
298             # If user inputs less than 3 precursors, change
299             # speeds list to include
300             if int(mots) < int(max_precur_num):
301                 dif = int(max_precur_num) - int(mots)
302                 for g in range(dif):
303                     speeds = speeds + ['0000']
304             if ok_cancel == 'OK':
305                 # if ok_cancel == ok just continue on with the
306                 # code
307                 # save Speeds and Precursors to Data File
308                 save_data(precur, speeds, mode)

```

```

301     # Check user inputted speed values for all
        precursors
302     if '' in speeds:
303         sg.popup_error("One or more Motor Values were
            not entered")
304         op = False
305         speeds = []
306         precur = []
307     # now to change our decimal values to motor
        values
308     # max_speed = 700
309     mot_speeds = []
310     val_ints = 0
311     speed_ints = 0
312     # print(len(speeds))
313     for p in range(len(speeds)):
314         # print(speeds[p])
315         # ie 0.3333*700 = 233.31
316         val = round(float(speeds[p]) * max_speed)
317         # = 233
318         val_ints = val_ints + val
319         speed_ints = speed_ints + float(speeds[p])
320         # print(p)
321         val = str(val)
322         # = '233'
323         g = len(val)
324         # g = 3
325         d = 4 - g
326         # d = 1
327         # generate zero string to add in front
328         # print(d)
329         for t in range(d):
330             # print(t)
331             if t + 1 == d:
332                 val = '-' + val
333             else:
334                 val = '0' + val
335         # 0233
336         mot_speeds = mot_speeds + [val]
337     # print(mot_speeds)
338     if val_ints > max_speed * 1.14:
339         # print(val_ints)
340         sg.popup_error('Input speeds exceed the
            maximum motor speed sum')
341         op = False
342     elif speed_ints < 0.9:
343         # print(speed_ints)

```

```

344         sg.popup_error('Input concentrations do not
345             sum to the minimum of 0.9')
346         op = False
347     else:
348         op = True
349         speeds = []
350         break
351     speeds = []
352     precur = []
353 else:
354     speeds = []
355     precur = []
356 if mode == ['Two Fluid Gradient'] or mode == ['Constant +
357     Two Fluid Gradient']:
358     op = True
359     # create speeds list which just grabs the exact
360     # values inputted for precursor speeds
361     # create list of precursors used
362     for k in range(mots):
363         kstr = str(k)
364         precur = precur + [values[f"-P{kstr[0]}-"]]
365     steps = values['-S0-']
366     max_percent = values['-S1-']
367     inputs = [steps, max_percent]
368     percent = 0
369     # Confirmation Message of Experiment Settings
370     if mode == ['Constant + Two Fluid Gradient']:
371         percent = values['-S2-']
372         inputs = [steps, percent, max_percent]
373         ok_cancel = sg.popup_ok_cancel("You set up an
374             experiment for " + str(precur) +
375             " with " + str(
376                 steps) + "
377                 steps, " + str(
378                 max_percent) +
379                 " Percentage
380                 Range, and " +
381                 str(percent) + "
382                 Percent of 3rd
383                 Precursor. Note
384                 that the
385                 constant
386                 precursor " +
387                 "MUST BE LOADED
388                 IN MOTOR C.
389                 Also, in the
390                 gradient MOTOR

```

```

374                                     B STARTS AT
375                                     THE HIGHER
376                                     PERCENTAGE.")
else:
377     ok_cancel = sg.popup_ok_cancel("You set up an
378     experiment for " + str(precursor) +
379     " with " + str(
380     steps) + "
381     steps, " + str(
382     max_percent) +
383     " Percentage
384     Range")
385
386 # If user inputs less than 3 precursors, change
387 # stopping list to have three values
388 # if int(mots) < int(max_precursor_num):
389     # dif = int(max_precursor_num) - int(mots)
390     # for g in range(dif):
391         # stopping = stopping + ['0000']
392 # in mode 2 #['s###', 's###', 's###']# becomes
393 # // mode ['steps', 'percent of third precursor',
394 # 'max percent of the gradient composition'] valve
395 # // for the max gradient percent and example
396 # is going from 25%-75% to 75-25 instead of 0-100 to
397 # 100-0
398 # // in this case the max percent will be 75 or
399 # 100
400 # // for the step numbers the max value is 999
401 # // for third precursor percentage the max
402 # value is 100
403 # // for max gradient percentage the max value
404 # is 100
405 # // #['0###', '0###', '0###']# where ### is an
406 # absolute percent ie 100 = 100%, 050 = 50%
407
408 if ok_cancel == 'OK':
409     # if ok_cancel == ok just continue on with the
410     # code
411     # Make the speeds vector
412     s = len(steps)
413     m = len(max_percent)
414     p = len(str(percent))
415     speeds_steps = str(steps)
416     speeds_max_percent = str(max_percent)
417     speeds_percent = str(percent)
418     for i in range(4-s):

```

```

403         speeds_steps = str(0) + str(speeds_steps)
404     # print(speeds_steps)
405     for i in range(4-m):
406         speeds_max_percent = str(0) + str(
407             speeds_max_percent)
408     for i in range(4-p):
409         speeds_percent = str(0) + str(speeds_percent)
410     speeds = [speeds_steps, speeds_percent,
411             speeds_max_percent]
412     # print(speeds)
413
414     # save Speeds and Precursors to Data File
415     save_data(precursor, speeds, mode)
416     # Checking values are in the right range
417     # Check user inputted speed values for all
418     precursors
419     if '' in inputs:
420         sg.popup_error("One or more Experiment
421             Parameters were not entered")
422         op = False
423         speeds = []
424         precursor = []
425     # Max step is 999
426     elif int(steps) > 999:
427         sg.popup_error("Steps must be less than or
428             equal to 999")
429         op = False
430     # Max 3rd percentage is 100
431     elif int(percent) > 25:
432         sg.popup_error("Maximum 3rd precursor
433             Percentage is 25")
434         op = False
435     # Max Percentage Range is 100
436     elif int(max_percent) > 100 or int(max_percent) <
437         60:
438         sg.popup_error("Maximum percentage range is
439             60 to 100")
440         op = False
441     else:
442         op = True
443         break
444     speeds = []
445     precursor = []
446
447     else:
448         speeds = []
449         precursor = []

```

```

442
443     if op:
444         window.close()
445         if mode == ['Batch']:
446             mot_speeds = str(mot_speeds)
447             glove_box('batch_window', mots, def_mots, mot_speeds,
448                       stopping, max_precur_num, max_speed, mode)
449         else:
450             speeds = str(speeds)
451             print(speeds)
452             glove_box('batch_window', mots, def_mots, speeds,
453                       stopping, max_precur_num, max_speed, mode)
454             # print(mot_speeds)
455
456     else:
457         window.close()
458         return op
459     window.close()
460
461 def glove_box(experiment, number, def_mots, speeds, stopping,
462              max_precur_num, max_sp, mode):
463     max_speed = int(max_sp)
464     # print(speeds)
465     q = 3
466     refills = []
467     layoutrefill = []
468     for j in range(number):
469         jstr = str(j)
470         layoutrefill = layoutrefill + [[sg.Button(f"Fill Precursor {
471             jstr[0]}", size=(25, q))]]
472         refills = refills + [f"Fill Precursor {jstr[0]}"]
473     refills = refills + ["Fill All Precursors"]
474     layoutrefill = layoutrefill + [[sg.Button("Fill All Precursors",
475         size=(25, q))],
476                                     [sg.Button("Turn on Valve", size
477         =(25, 1))],
478                                     [sg.Button("Recalibrate Syringes",
479         size=(25, q + 1), button_color
480         ='purple')],
481                                     [sg.Button("Stop Print and Exit",
482         size=(25, q), button_color='red
483         ')]]
484
485     # print(layoutrefill)
486     layoutss = [[sg.Button("Start Batch Print", s=(25, 25),
487         button_color='green'),
488                 sg.VSeparator(),

```

```

477         sg.Button("Stop All", s=(25, 25), button_color='
           orange')]]
478
479 layout = [[sg.Column(layoutss), sg.VSeparator(), sg.Column(
           layoutrefill)]]
480
481 window_title = 'Glove Box Controls'
482 window = sg.Window(window_title, layout)
483 # number is the number of motors or precursors
484 # change speeds to a list that the arduino can read
485 # stopspeeds = "['0000', '0000', '0000']0"
486 stopspeeds = str(1) + str(stopping) + str(0)
487 # print(stopspeeds)
488 if mode == ['Batch']:
489     startspeeds = str(1) + speeds + str(1)
490 else:
491     startspeeds = str(2) + speeds + str(1)
492 # print(startspeeds)
493 # build vector with equal speeds for all motors
494 rat = 1 / number
495 w = []
496 w_speeds = []
497 # w for warm-up
498 for j in range(number):
499     w = w + [rat]
500 for p in range(number):
501     # print(speeds[p])
502     # ie 0.3333*700 = 233.31
503     val = round(float(w[p]) * max_speed)
504     # = 233
505     # print(p)
506     val = str(val)
507     # = '233'
508     g = len(val)
509     # g = 3
510     d = 4 - g
511     # d = 1
512     # generate zero string to add in front
513     # print(d)
514     for t in range(d):
515         # print(t)
516         if t + 1 == d:
517             val = '-' + val
518         else:
519             val = '0' + val
520     # 0233
521     w_speeds = w_speeds + [val]

```

```

522     for k in range(max_precur_num-number):
523         w_speeds = (w_speeds + ['0000'])
524     w_speeds = str(1) + str(w_speeds) + str(1)
525
526     while True:
527         event, values = window.read()
528         if event == sg.WINDOW_CLOSED:
529             break
530         if event == "Turn on Valve":
531             i = str(1) + str(stopping) + str(1)
532             while True:
533                 serialcomm.write(i.encode())
534                 time.sleep(0.5)
535             break
536         if event == "Recalibrate Syringes":
537             i = []
538             for k in range(number):
539                 i = i + ['-050']
540             if number < max_precur_num:
541                 for l in range(max_precur_num - number):
542                     i = i + ['0000']
543             i = str(1) + str(i) + str(1)
544             print(i)
545             while True:
546                 serialcomm.write(i.encode())
547                 time.sleep(0.5)
548             break
549             time.sleep(20)
550             i = str(1) + str(stopping) + str(0)
551             while True:
552                 serialcomm.write(i.encode())
553                 time.sleep(0.5)
554             break
555
556         if event == 'Stop All':
557             i = stopping
558             i = str(1) + str(i) + '0'
559             while True:
560                 serialcomm.write(i.encode())
561                 time.sleep(0.5)
562             break
563
564         if event in refills:
565             # print(event)
566             i = []
567             if event == "Fill All Precursors":
568                 for k in range(number):

```

```

569         i = i + ['0600']
570     else:
571         wvent = str(event)
572         for k in range(number):
573             if k == int(wvent[15]):
574                 # building the serial message as ['####', '
                    ####', '####']0
575                 # if you are at the location within the
                    message for the motor you want to
                    communicate with
576                 # make the speed 500, else make the speed 0
577                 i = i + ['0600']
578                 # print(k)
579             else:
580                 i = i + ['0000']
581         for f in range(max_precur_num - number):
582             i = i + ['0000']
583         i = str(i)
584         i = str(1) + i + '0'
585         # print(i)
586         # print(wvent[15])
587         while True:
588             serialcomm.write(i.encode())
589             time.sleep(0.5)
590             break
591     if event == 'Stop Print and Exit':
592         while True:
593             i = stopspeeds
594             serialcomm.write(i.encode())
595             time.sleep(0.5)
596             break
597             # print
598         number = str(number)
599         def_mots = str(def_mots)
600         window.close()
601         # print(number)
602         eval(experiment + f'("{number}", f"{def_mots}", f"{str(
                    max_precur_num)}", f"{max_speed}", f"{mode}")')
603         break
604     if event == 'Start Batch Print':
605         # first run all the motors at same speed for 25 seconds
606         # then run the given speed/settings values
607         while True:
608             i = w_speeds
609             serialcomm.write(i.encode())
610             time.sleep(0.5)
611             break

```

```

612         time.sleep(7)
613         while True:
614             i = startspeeds
615             print(i)
616             serialcomm.write(i.encode())
617             time.sleep(0.5)
618             break
619             # print(serialcomm.readline().decode('ascii'))
620 window.close()
621
622
623 if __name__ == "__main__":
624     default_motors = 3
625     max_precursors = 3
626     max_speed = 400
627     # Changed from 700 to 400 because of over pressurization issues
628     # Gets set-up choices and checks that the user wants to continue
        with them
629     con = True
630     while True:
631         if con:
632             choices, moto, con, max_precur_num = setup_window(
                default_motors, max_precursors)
633             if con == 'Cancel':
634                 # print("Con was non")
635                 con = True
636             else:
637                 if not len(choices) == 0:
638                     op = batch_window(moto, default_motors,
                        max_precur_num, max_speed, choices)
639                     if not op:
640                         con = True
641                 else:
642                     sg.popup_error("Not Yet Defined")

```


Appendix C

Archerfish Arduino Code

```
1 // Version 1 Python to Arduino Serial communication motor control
  Code
2 // Author Eunice Aissi on 9/9/2022
3 int trans = 22;
4 // Variables for running Serial Communication
5 char mode;
6 String incomingByte;
7 // Mode 2 Gradient + Constant solvent mode
8 char step1;
9 char step2;
10 char step3;
11 char prec_per1;
12 char prec_per2;
13 char prec_per3;
14 char grad_max1;
15 char grad_max2;
16 char grad_max3;
17 int step100;
18 int step10;
19 int stepone;
20 int prec_per100;
21 int prec_per10;
22 int prec_perone;
23 int grad_max100;
24 int grad_max10;
25 int grad_maxone;
26 int steps;
27 int prec_per;
28 int grad_max;
29 int maxStepSpeed = 500; // max stepSpeed = 800 before failure/
  unreliable
30 int precursor_range = 50; // previously 300
31 int gradient_range = maxStepSpeed - precursor_range;
32 // Mode 1 Batch Mode
```

```

33 char speedA1;
34 char speedA2;
35 char speedA3;
36 char speedB1;
37 char speedB2;
38 char speedB3;
39 char speedC1;
40 char speedC2;
41 char speedC3;
42 char Sign1;
43 char Sign2;
44 char Sign3;
45 char valve;
46 int speedA100;
47 int speedA10;
48 int speedAone;
49 int speedB100;
50 int speedB10;
51 int speedBone;
52 int speedC100;
53 int speedC10;
54 int speedCone;
55 int speedA;
56 int speedB;
57 int speedC;
58
59 //Variables for runing motors copied from Aleks' 2_motor_Step_V4_AS
   code
60
61
62 // Stepper A pins
63 int a1 = 10;
64 int a2 = 11;
65 int a3 = 12;
66 int a4 = 13;
67 // Stepper B pins
68 int b1 = 2;
69 int b2 = 3;
70 int b3 = 4;
71 int b4 = 5;
72 //Stepper C pins - added by Eunice
73 int c1 = 6;
74 int c2 = 7;
75 int c3 = 8;
76 int c4 = 9;
77
78

```

```

79 // always choose a maxStepSpeet value that is divisible by 10!!!!
80 int stepAccel = 100; // don't really need to change this acceleration
    value
81 int stepTime =10; // seconds. don't exceed 30 seconds or it will run
    forever
82         // motors run for stepTime*(number of motors)
83 int stepDirection = -1; // -1 for CW (plunger goes down) and 1 for
    CCW (plunger goes up) [motor pin facing down]
84 char firstMotor = 'A'; // 'A' => first, motor A runs for stepTime
    then turns off and motor B runs for stepTime
85         // 'B' => first, motor B runs for stepTime
            then turns off and motor A runs for
            stepTime
86
87 float increment ;
88 // for Gradient + constant mode
89 unsigned long wait_time;
90 unsigned long purge_time;
91 unsigned long begin_time2;
92
93 #include <AccelStepper.h> // Tools > Manage Libraries ... > search
    for and install AccelStepper
94 #define HALFSTEP 8 // number of full steps for 28BYJ-48 stepper
    motors
95 AccelStepper stepperA(HALFSTEP,a1,a3,a2,a4); // define stepper 1 pins
96 AccelStepper stepperB(HALFSTEP,b1,b3,b2,b4); // define stepper 2 pins
97 AccelStepper stepperC(HALFSTEP,c1,c3,c2,c4); // define stepper 3 pins
    - added by Eunice
98 // motor controller pin map out (FULLSTEP, N1, N3, N2, N4) Npins are
    the motor controller pins
99 int buffer_time = 22000;
100
101 void setup() {
102     // put your setup code here, to run once:
103     // Serial communication set up
104     Serial.begin(9600);
105     pinMode(LED_BUILTIN, OUTPUT);
106     pinMode(trans, OUTPUT);
107
108     // Motor Control Setup
109     // Stepper 1 settings
110     stepperA.setMaxSpeed(maxStepSpeed);
111     stepperA.setAcceleration(stepAccel);
112     // Stepper 2 settings
113     stepperB.setMaxSpeed(maxStepSpeed);
114     stepperB.setAcceleration(stepAccel);
115     // Stepper 3 settings

```

```

116     stepperC.setMaxSpeed(maxStepSpeed);
117     stepperC.setAcceleration(stepAccel);
118 }
119 void loop() {
120     // put your main code here, to run repeatedly:
121     while (Serial.available()>0) {
122         incomingByte = Serial.readStringUntil('/n'); // read till end of
            line
123         incomingByte.trim();
124         //Serial.print(incomingByte);
125         // Save input values as speed values
126         // input speed values #[ 's###', 's###', 's###' ]#
127         // input mode[speed motor A, speed motor B, speed motor C]valve
            on/off
128         // extract individual charcaters note zero indexing
129         //Serial.print(incomingByte);
130         valve    = incomingByte.charAt(25);
131         mode     = incomingByte.charAt(0);
132         if (valve == '1') {
133             digitalWrite(trans, HIGH);
134         }
135         if (valve == '0') {
136             digitalWrite(trans, LOW);
137         }
138         // mode one batch mode input speed values and run those speeds
139         if (mode == '1'){
140             speedA1 = incomingByte.charAt(4);
141             speedA2 = incomingByte.charAt(5);
142             speedA3 = incomingByte.charAt(6);
143             speedB1 = incomingByte.charAt(12);
144             speedB2 = incomingByte.charAt(13);
145             speedB3 = incomingByte.charAt(14);
146             speedC1 = incomingByte.charAt(20);
147             speedC2 = incomingByte.charAt(21);
148             speedC3 = incomingByte.charAt(22);
149             Sign1   = incomingByte.charAt(3);
150             Sign2   = incomingByte.charAt(11);
151             Sign3   = incomingByte.charAt(19);
152
153             // turn them into integers and multiply by their place value
154             String speedA1s = String(speedA1);
155             String speedA2s = String(speedA2);
156             String speedA3s = String(speedA3);
157             String speedB1s = String(speedB1);
158             String speedB2s = String(speedB2);
159             String speedB3s = String(speedB3);
160             String speedC1s = String(speedC1);

```

```

161     String speedC2s = String(speedC2);
162     String speedC3s = String(speedC3);
163
164     speedA100 = 100* speedA1s.toInt() ;
165     speedA10  = 10*  speedA2s.toInt() ;
166     speedAone = 1*   speedA3s.toInt() ;
167     speedB100 = 100* speedB1s.toInt() ;
168     speedB10  = 10*  speedB2s.toInt() ;
169     speedBone = 1*   speedB3s.toInt() ;
170     speedC100 = 100* speedC1s.toInt() ;
171     speedC10  = 10*  speedC2s.toInt() ;
172     speedCone = 1*   speedC3s.toInt() ;
173     //add them to make the final speed
174     speedA = speedA100 + speedA10 + speedAone;
175     speedB = speedB100 + speedB10 + speedBone;
176     speedC = speedC100 + speedC10 + speedCone;
177     //Serial.println(speedA);
178     if (Sign1 == '-') {
179         speedA = speedA * -1;
180     }
181     if (Sign2 == '-') {
182         speedB = speedB * -1;
183     }
184     if (Sign3 == '-') {
185         speedC = speedC * -1;
186     }
187
188     //input check to make sure the sum of speeds doesn't exceed
189     // 100%
190     if (abs(speedA) + abs(speedB) + abs(speedC) > maxStepSpeed) { //
191         // need to change this to absolute value
192         Serial.print("Invalid Input");
193     }
194     stepperA.setSpeed(speedA);
195     stepperB.setSpeed(speedB);
196     stepperC.setSpeed(speedC);
197 } // End of Mode 1
198
199 if (mode == '2') {
200     // mode 2, two motor making a gradient, third motor is constant
201     // need increment for gradient and motor 3 speed
202     // in mode 2 #['s###', 's###', 's###']# becomes
203     // mode ['steps', 'percent of third precursor', 'max percent of
204     // the gradient composition'] valve
205     // for the max gradient percent and example is going from
206     // 25%-75% to 75-25 instead of 0-100 to 100-0
207     // in this case the max percent will be 75 or 100

```

```

204 // for the step numbers the max value is 999
205 // for third precursor percentage the max value is 100
206 // for max gradient percentage the max value is 100
207 // #['0###', '0###', '0###']# where ### is an absolute percent
      ie 100 = 100%, 050 = 50%
208 // Extract the info you need, note that chafcaters are 0 indexed
      , spaces are characters
209 step1 = incomingByte.charAt(4);
210 step2 = incomingByte.charAt(5);
211 step3 = incomingByte.charAt(6);
212 prec_per1 = incomingByte.charAt(12);
213 prec_per2 = incomingByte.charAt(13);
214 prec_per3 = incomingByte.charAt(14);
215 grad_max1 = incomingByte.charAt(20);
216 grad_max2 = incomingByte.charAt(21);
217 grad_max3 = incomingByte.charAt(22);
218 // turn them into integers and multiply by their place value
219 String step1s = String(step1);
220 String step2s = String(step2);
221 String step3s = String(step3);
222 String prec_per1s = String(prec_per1);
223 String prec_per2s = String(prec_per2);
224 String prec_per3s = String(prec_per3);
225 String grad_max1s = String(grad_max1);
226 String grad_max2s = String(grad_max2);
227 String grad_max3s = String(grad_max3);
228
229 step100 = 100* step1s.toInt() ;
230 step10  = 10*  step2s.toInt() ;
231 stepone = 1*  step3s.toInt() ;
232 prec_per100 = 100* prec_per1s.toInt() ;
233 prec_per10  = 10*  prec_per2s.toInt() ;
234 prec_perone = 1*  prec_per3s.toInt() ;
235 grad_max100 = 100* grad_max1s.toInt() ;
236 grad_max10  = 10*  grad_max2s.toInt() ;
237 grad_maxone = 1*  grad_max3s.toInt() ;
238
239 steps =step100 + step10 + stepone;
240 prec_per = prec_per100 + prec_per10 + prec_perone;
241 grad_max = grad_max100 + grad_max10 + grad_maxone;
242 wait_time = 250;
243 purge_time = 20000;
244 mode2(steps,prec_per,grad_max,wait_time, begin_time2,
      maxStepSpeed, buffer_time, stepDirection, purge_time);
245 } // end of Mode 2
246
247 } // while ends

```

```

248
249     stepperA.runSpeed();
250     stepperB.runSpeed();
251     stepperC.runSpeed();
252 } // End of Void Loop
253
254 // START of Special Functions
255
256
257 void mode2 (int steps, int prec_per, int grad_max, unsigned long
    wait_time, unsigned long begin_time2, int maxStepSpeed,
258 int buffer_time, int stepDirection, unsigned long purge_time) {
259     // first step is determining the speed bounds based on the
260     // max percent of the gradient composition and precursor percentage
261     float prec_per_float = prec_per; // prec_per = % solvent
262     float C = (prec_per_float/100);
263     // because percentage of solvent = Solvent speed/ ( solvent speed +
        precursor total speed)
264     // solve that solvent speed for a given percentage of solvent
        composition is  $S = CP/(1-C)$  where C is desired percent
        composition, P is precursor total speed, and S is solvent speed
265     // this makes for a maximum of 25% is solvent composition.
266     float stepperC_speed = ( C * precursor_range)/(1-C); // precursor
        range refers to MA/FA
267     // 2['0100', '0050', '0100']0
268     float max_gradient_speed = precursor_range;
269     float grad_max_float = grad_max;
270     float max_gradient_comp_speed = max_gradient_speed * (
        grad_max_float/100); // max speed based on the gradient
        composition
271     // ie. the maximum speed of the starting motor for the 75-25
        composition start point
272     float min_gradient_comp_speed = max_gradient_speed -
        max_gradient_comp_speed;
273     // now find the increment
274     float step_float = steps;
275     float increment = (max_gradient_comp_speed -
        min_gradient_comp_speed)/step_float;
276     float speedq = 0;
277     stepperA.setSpeed(stepDirection * min_gradient_comp_speed);
278     stepperB.setSpeed(stepDirection * max_gradient_comp_speed);
279     stepperC.setSpeed(stepDirection * stepperC_speed); // replaced
        stepperC_speed with 800 worked
280     begin_time2 = millis();
281     while (millis()-begin_time2 < buffer_time ){
282         // run motor speeds
283         stepperA.runSpeed();

```

```

284     stepperB.runSpeed();
285     stepperC.runSpeed();
286 }
287 for (int i=0; i<steps+1; i+=1){
288     if (i<steps){
289         speedq = speedq + increment ;
290         stepperA.setSpeed(stepDirection * speedq);
291         stepperB.setSpeed(stepDirection * (max_gradient_speed - speedq)
292             );
293         unsigned long begin_time = millis();
294         while (millis()-begin_time < wait_time ){
295             // run motor speeds
296             stepperA.runSpeed();
297             stepperB.runSpeed();
298             stepperC.runSpeed();
299         }
300     }
301     else if (i>=steps){
302         unsigned long begin_time = millis();
303         while (millis()-begin_time < purge_time ){
304             // run motor speeds
305             stepperA.runSpeed();
306             stepperB.runSpeed();
307             stepperC.runSpeed();
308         }
309     }
310     stepperA.setSpeed(0);
311     stepperB.setSpeed(0);
312     stepperC.setSpeed(0);
313     digitalWrite(trans, LOW);
314 }

```

References

- [1] J.-P. Correa-Baena, K. Hippalgaonkar, J. van Duren, S. Jaffer, V. R. Chandrasekhar, V. Stevanovic, C. Wadia, S. Guha, and T. Buonassisi. “Accelerating Materials Development via Automation, Machine Learning, and High-Performance Computing”. In: *Joule* 2 (8 Aug. 2018), pp. 1410–1420. ISSN: 2542-4785. DOI: [10.1016/j.joule.2018.05.009](https://doi.org/10.1016/j.joule.2018.05.009).
- [2] A. E. Siemenn. *A System for High-Throughput Materials Exploration Driven by Machine Learning*. 2021.
- [3] R. M. Hazen. “Perovskites”. In: *Scientific American* 258.6 (1988), pp. 74–81. ISSN: 00368733, 19467087. URL: <http://www.jstor.org/stable/24989124> (visited on 08/23/2024).
- [4] L. Ortega-San-Martin. “Introduction to Perovskites: A Historical Perspective”. In: *Revolution of Perovskite: Synthesis, Properties and Applications*. Ed. by N. S. Arul and V. D. Nithya. Singapore: Springer Singapore, 2020, pp. 1–41. ISBN: 978-981-15-1267-4. DOI: [10.1007/978-981-15-1267-4_1](https://doi.org/10.1007/978-981-15-1267-4_1). URL: https://doi.org/10.1007/978-981-15-1267-4_1.
- [5] L. Zhang et al. “Advances in the Application of Perovskite Materials”. In: *Nano-Micro Letters* 15 (1 Aug. 2023), p. 177. ISSN: 2150-5551. DOI: [10.1007/s40820-023-01140-3](https://doi.org/10.1007/s40820-023-01140-3).
- [6] X. Fan. “Advanced progress in metal halide perovskite solar cells: A review”. In: *Materials Today Sustainability* 24 (2023), pp. 100–603. ISSN: 2589-2347. DOI: <https://doi.org/10.1016/j.mtsust.2023.100603>. URL: <https://www.sciencedirect.com/science/article/pii/S2589234723002907>.
- [7] Y. Rong, Y. Hu, A. Mei, H. Tan, M. I. Saidaminov, S. I. Seok, M. D. McGehee, E. H. Sargent, and H. Han. “Challenges for commercializing perovskite solar cells”. In: *Science* 361.6408 (2018), eaat8235. DOI: [10.1126/science.aat8235](https://doi.org/10.1126/science.aat8235). eprint: <https://www.science.org/doi/pdf/10.1126/science.aat8235>. URL: <https://www.science.org/doi/abs/10.1126/science.aat8235>.
- [8] A. E. Siemenn, E. Aissi, F. Sheng, A. Tiihonen, H. Kavak, B. Das, and T. Buonassisi. “Using scalable computer vision to automate high-throughput semiconductor characterization”. In: *Nature Communications* 15.1 (2024), p. 4654.
- [9] F. F. Targhi, Y. S. Jalili, and F. Kanjouri. “MAPbI₃ and FAPbI₃ perovskites as solar cells: Case study on structural, electrical and optical properties”. In: *Results in Physics* 10 (2018), pp. 616–627. ISSN: 2211-3797. DOI: <https://doi.org/10.1016/j.rinp.2018.07.007>. URL: <https://www.sciencedirect.com/science/article/pii/S2211379718311811>.
- [10] S. Sun et al. “A data fusion approach to optimize compositional stability of halide perovskites”. In: *Matter* 4.4 (2021), pp. 1305–1322. DOI: [10.1016/j.matt.2021.01.008](https://doi.org/10.1016/j.matt.2021.01.008).

- [11] Z. A. Nan et al. “Revealing phase evolution mechanism for stabilizing formamidinium-based lead halide perovskites by a key intermediate phase”. In: *Chem* 7 (9 Sept. 2021), pp. 2513–2526. ISSN: 2451-9294. DOI: [10.1016/J.CHEMPR.2021.07.011](https://doi.org/10.1016/J.CHEMPR.2021.07.011).
- [12] J. Wu, J. Chen, and H. Wang. “Phase Transition Kinetics of MAPbI₃ for Tetragonal-to-Orthorhombic Evolution”. In: *JACS Au* 3 (4 Apr. 2023), pp. 1205–1212. ISSN: 26913704. DOI: [10.1021/JACSAU.3C00060/SUPPL_FILE/AU3C00060_SI_002.ZIP](https://doi.org/10.1021/JACSAU.3C00060/SUPPL_FILE/AU3C00060_SI_002.ZIP).
- [13] R. Keeseey et al. “An open-source environmental chamber for materials-stability testing using an optical proxy”. In: *Digit. Discov.* (2023). ISSN: 2635-098X. DOI: [10.1039/D2DD00089J](https://doi.org/10.1039/D2DD00089J).
- [14] P. Menesatti, C. Angelini, F. Pallottino, F. Antonucci, J. Aguzzi, and C. Costa. “RGB Color Calibration for Quantitative Image Analysis: The “3D Thin-Plate Spline” Warping Approach”. In: *Sensors* 12.6 (2012), pp. 7063–7079. ISSN: 1424-8220. DOI: [10.3390/s120607063](https://doi.org/10.3390/s120607063).
- [15] C. C. Stoumpos, L. Mao, C. D. Malliakas, and M. G. Kanatzidis. “Structure-Band Gap Relationships in Hexagonal Polytypes and Low-Dimensional Structures of Hybrid Tin Iodide Perovskites”. In: *Inorg. Chem.* 56 (1 Jan. 2017), pp. 56–73. ISSN: 1520510X. DOI: [10.1021/ACS.INORGCHEM.6B02764/SUPPL_FILE/IC6B02764_SI_013.CIF](https://doi.org/10.1021/ACS.INORGCHEM.6B02764/SUPPL_FILE/IC6B02764_SI_013.CIF).
- [16] B. Charles, J. Dillon, O. J. Weber, M. S. Islam, and M. T. Weller. “Understanding the stability of mixed A-cation lead iodide perovskites”. In: *J. Mater. Chem. A* 5 (43 Nov. 2017), pp. 22495–22499. ISSN: 20507496. DOI: [10.1039/C7TA08617B](https://doi.org/10.1039/C7TA08617B).
- [17] O. J. Weber, B. Charles, and M. T. Weller. “Phase behaviour and composition in the formamidinium–methylammonium hybrid lead iodide perovskite solid solution”. In: *J. Mater. Chem. A* 4 (40 Oct. 2016), pp. 15375–15382. ISSN: 2050-7496. DOI: [10.1039/C6TA06607K](https://doi.org/10.1039/C6TA06607K).
- [18] A. Pisanu, C. Ferrara, P. Quadrelli, G. Guizzetti, M. Patrini, C. Milanese, C. Tealdi, and L. Malavasi. “The FA1–xMAxPbI₃ System: Correlations among Stoichiometry Control, Crystal Structure, Optical Properties, and Phase Stability”. In: *J. Phys. Chem. C* 121 (16 Apr. 2017), pp. 8746–8751. ISSN: 1520-5215. DOI: [10.1021/acs.jpcc.7b01250](https://doi.org/10.1021/acs.jpcc.7b01250).
- [19] A. Binek, F. C. Hanusch, P. Docampo, and T. Bein. “Stabilization of the Trigonal High-Temperature Phase of Formamidinium Lead Iodide”. In: *J. Phys. Chem. Lett.* 6 (7 Apr. 2015), pp. 1249–1253. ISSN: 1948-7185. DOI: [10.1021/acs.jpcclett.5b00380](https://doi.org/10.1021/acs.jpcclett.5b00380).
- [20] A. Siemenn, B. Das, E. Aissi, F. Sheng, L. Elliot, B. Hudspeth, M. Meyers, J. Serdy, and T. Buonassisi. “A Retrofitted 3D Printer for High-throughput Combinatorial Experimentation via Continuous Printing.” In: *ChemRxiv* (2024). DOI: [10.26434/chemrxiv-2024-fz16p](https://doi.org/10.26434/chemrxiv-2024-fz16p).
- [21] R. Sliz, J. Czajkowski, and T. Fabritius. “Taming the Coffee Ring Effect: Enhanced Thermal Control as a Method for Thin-Film Nanopatterning”. In: *Langmuir* 36.32 (2020), pp. 9562–9570.